Journal of Medicinal Chemistry

ARTICLE

pubs.acs.org/jmc

Synthesis and Biochemical Evaluation of Δ^2-Isoxazoline Derivatives as DNA Methyltransferase 1 Inhibitors

Sabrina Castellano,[†,⊥] Dirk Kuck,[*,‡,⊥] Monica Viviano,[†] Jakyung Yoo,[§] Fabian López-Vallejo,[§] Paola Conti,[∥] Lucia Tamborini,[∥] Andrea Pinto,[∥] José L. Medina-Franco,[*,§] and Gianluca Sbardella[*,†]

[†]Dipartimento di Scienze Farmaceutiche e Biomediche, Epigenetic Med Chem Lab, Università degli Studi di Salerno, Via Ponte Don Melillo, I-84084 Fisciano (SA), Italy

[‡]Division of Epigenetics, DKFZ-ZMBH Alliance, German Cancer Research Center, Im Neuenheimer Feld 580, 69120 Heidelberg, Germany

[§]Torrey Pines Institute for Molecular Studies, 11350 SW Village Parkway, Port St. Lucie, Florida 34987, United States

[∥]Dipartimento di Scienze Farmaceutiche "Pietro Pratesi", Università degli Studi di Milano, Via Mangiagalli 25, 20133 Milano, Italy

Supporting Information

ABSTRACT: A series of Δ^2-isoxazoline constrained analogues of procaine/procainamide (**7a**−**k** and **8a**−**k**) were prepared and their inhibitory activity against DNA methyltransferase 1 (DNMT1) was tested. Among them, derivative **7b** is far more potent in vitro (IC_{50} = 150 μM) than other non-nucleoside inhibitors and also exhibits a strong and dose-dependent antiproliferative effect against HCT116 human colon carcinoma cells. The binding mode of **7b** with the enzyme was also investigated by means of a simple competition assay as well as of docking simulations conducted using the recently published crystallographic structure of human DNMT1. On the basis of the findings, we assessed that the mode of inhibition of **7b** is consistent with a competition with the cofactor and propose it as a novel lead compound for the development of non-nucleoside DNMT inhibitors.

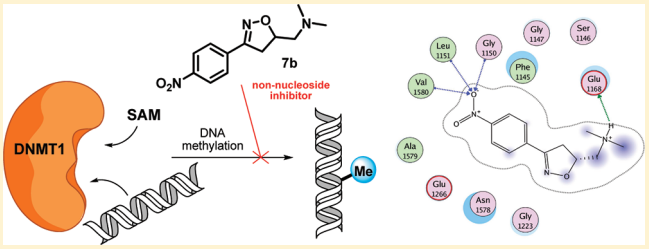

INTRODUCTION

Epigenetic mechanisms are essential for normal development and maintenance of tissue-specific gene expression patterns in mammals. As a whole, these modifications create an "epigenetic landscape", alteration or disruption of which is a hallmark of virtually all cases of cancer.[1−7] Both genetic and epigenetic events regulate the onset of cancer,[8,9] but unlike genetic mutations, epigenetic aberrations are potentially reversible and can be restored to their normal state.[10,11] This makes epigenetic therapy a promising and valuable approach to chemotherapy as well as chemoprevention of cancer.

Probably, the most extensively studied epigenetic modification in humans is the addition of a methyl group at the carbon-5 position of cytosine residues.[12] DNA methylation in humans occurs almost exclusively in the context of CpG dinucleotides[13] clustered in ∼1 kb regions, termed CpG islands.[4,14] In addition, it also occurs at regions of lower CpG density that lie in close proximity (∼2 kb), termed "CpG island shores".[15,16]

In general, DNA methylation is associated with transcriptional silencing of genes implicated in the pathogenesis of many diseases including cancer.[4,8,17−21] Establishment and maintenance of DNA methylation patterns are governed by catalytically active DNA methyltransferase (DNMT) enzymes.

To date, three[22] active DNMTs have been identified in humans. DNMT1 is the most abundant among the three and is responsible for the maintenance of CpG methylation patterns in mammals with hemimethylated CpG dinucleotides serving as preferred substrates.[23] The DNMT3 isoforms (DNMT3A and DNMT3B) are responsible for de novo methylation during germ cell and embryonic development, thus being able to use hemimethylated as well as unmethylated DNA sequences as substrates. It has been shown that the inhibition of DNA methyltransferase activity can lead to demethylation and reactivation of epigenetically silenced tumor suppressor genes[24] and, indeed, DNA methylation inhibitors were the first successful epigenetic drugs developed and used as cancer therapeutics.

Two types of DNMT inhibitors have been hitherto described (Chart 1).[11,25] Nucleoside analogues, such as the U.S. Food and Drug Administration (FDA)-approved 5-azacytidine (5-aza-CR, Vidaza, Calgene) and 5-aza-2′-deoxycytidine (5-aza-CdR, decitabine, Dacogen, Supergen), or 2-pyrimidone-1-β-D-riboside (zebularine), or the recently discovered dinucleotide derivative **1** (SGI-110),[26,27] exert their effects by incorporation into DNA inducing substantial DNA demethylation and reactivation of hypermethylated genes. Yet, they also carry considerable concerns about toxicity. Their use, in fact, is associated with increased incidence of bone marrow suppression, including

Received: August 3, 2011
Published: September 29, 2011

neutropenia and thrombocytopenia,[11,28−31] even if the tolerability of **1** seems to be more favorable.[27]

Because of these concerns, the search and the development of non-nucleoside compounds, which can effectively inhibit DNA methylation without being incorporated into DNA, is being actively pursued.[1,11] Differently from nucleoside analogues, non-nucleoside inhibitors exhibit a wide structural diversity (Chart 2), as they include dietary polyphenols like (−)-epigallocatechin-3-gallate (EGCG),[32] curcumin,[33] apple polyphenols,[34] caffeic and chlorogenic acids,[35] the soy bean isoflavone genistein,[36] the bisulfide bromotyrosine derivatives psammaplins,[37] the L-tryptophan derivative **2** (RG108)[38,39] and related maleimide derivatives,[40] the antibiotic nanaomycin A[41] and mithramycin A,[42] constrained analogues of *S*-adenosylhomocysteine (SAH),[43,44] the sulfonamide IM-25,[45] the quinoline derivative SGI-1027,[46] the vasodilatator hydralazine,[47,48] the 4-aminobenzoic acid derivatives procaine and procainamide,[49−52] as well as other compounds.[53,54]

It is worth noting that few efforts have been conducted so far with non-nucleoside inhibitors to elucidate experimentally the kinetics and specific mode of inhibition.

Being interested in the development of small-molecule modulators of epigenetic targets,[38,39,41,48,53−72] we focused our attention on procaine/procainamide as a lead structure for further modification. Originally approved by the FDA as local anesthetic and antiarrhythmic drug, respectively, procaine and procainamide have emerged as potential DNA demethylating agents.[45,51] It has been reported that procainamide specifically inhibits DNMT1 by reducing the affinity with hemimethylated DNA (substrate) and *S*-adenosylmethionine (cofactor),[49,52,73] thus causing growth arrest[51] and reactivation of tumor suppressor genes in cancer cells.[74] With the aim to increase potency, according to the frozen analogue approach, we decided to limit the very high flexibility of procaine/procainamide scaffold by constraining the *N*-alkylamide moiety into a 4-substituted- or 5-substituted-oxazoline ring (derivatives **3**,**4** and **5**,**6**, Figure 1).[55] Among the synthesized compounds, unexpectedly, the nitro derivative **5b** (Chart 2

Chart 1. Nucleoside Inhibitors of DNMTs

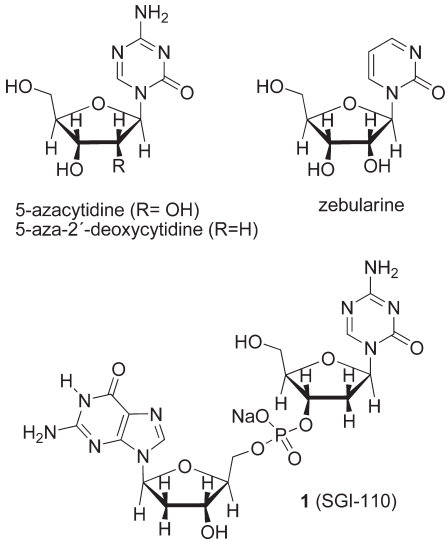

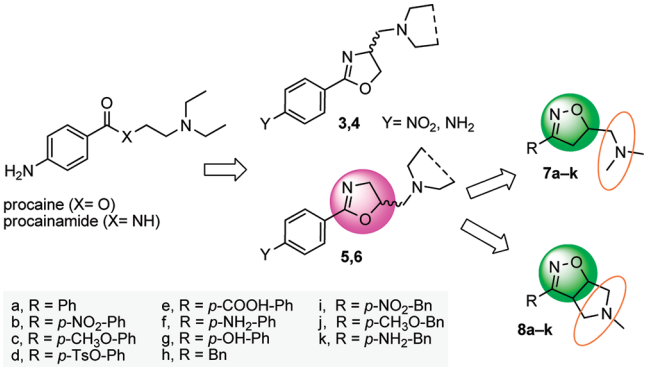

Figure 1. Oxazoline derivatives **3**−**6** and Δ^2-isoxazoline derivatives **7a**−**k** and **8a**−**k**.

Chart 2. Non-nucleoside Inhibitors of DNMTs

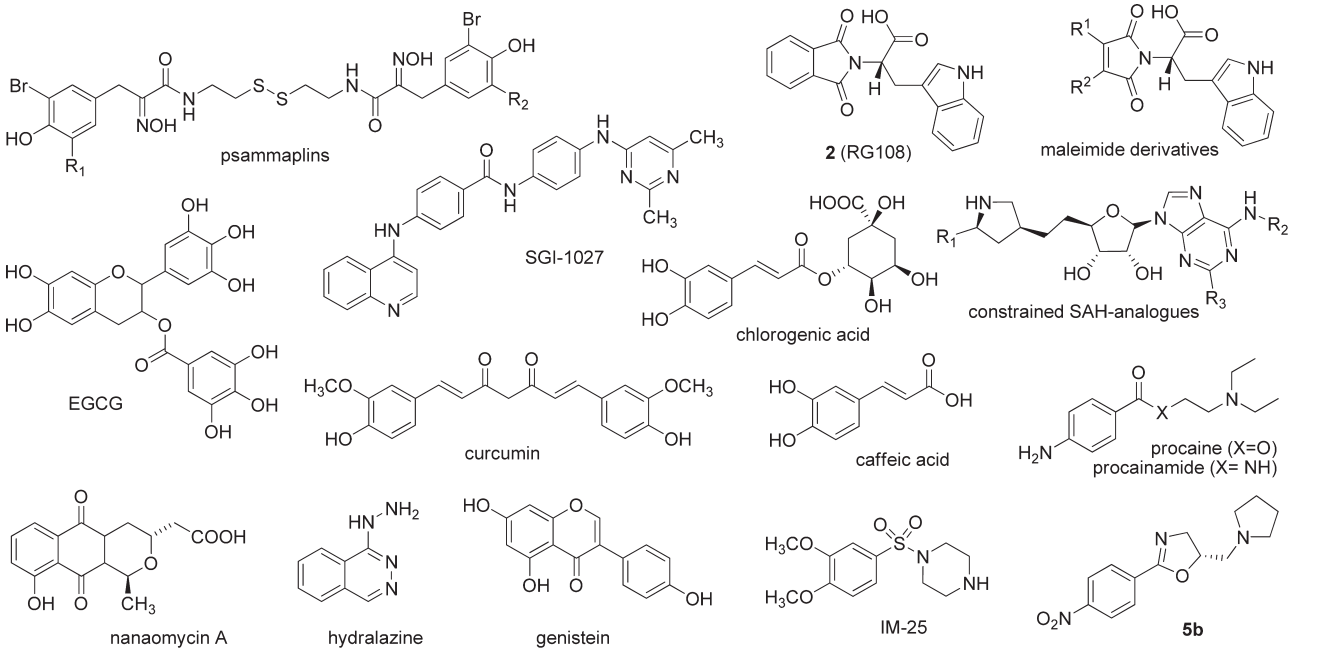

dx.doi.org/10.1021/jm2010404 |*J. Med. Chem.* 2011, 54, 7663–7677

Scheme 1. Synthesis of Δ^2-Isoxazolines 7a−k[a]

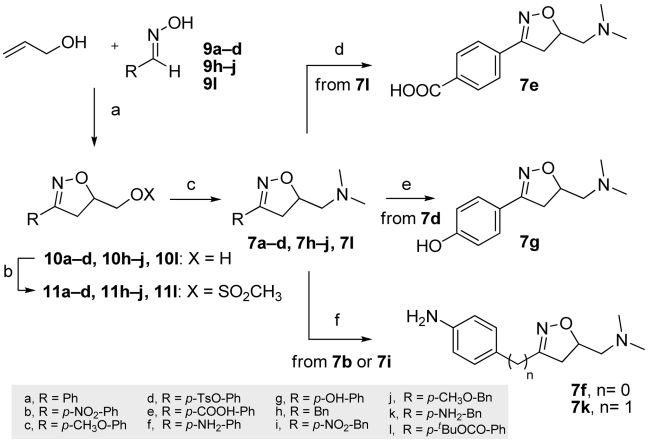

[a] Reagents and conditions: (a) 3% NaOCl, CH_2Cl_2, 0 °C to room temperature, 15 min; (b) MsCl, TEA, CH_2Cl_2, 0 °C to room temperature, 45 min; (c) dimethylamine, THF, 100 °C, sealed tube, 12 h; (d) TFA/CH_2Cl_2 1:3, room temperature, overnight; (e) 1N NaOH, EtOH, reflux, 1 h; (f) zinc powder, acetic acid, room temperature, 1 h.

Scheme 2. Synthesis of Δ^2-Isoxazolines 8a−k[a]

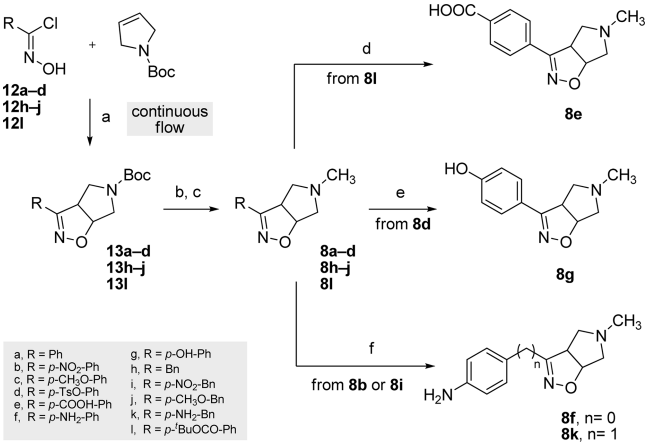

[a] Reagents and conditions: (a) R2/R4 flow reactor, EtOAc, K_2CO_3, 80 °C, 10 min; (b) 4N HCl, dioxane, room temperature, 1 h; (c) CH_3I, K_2CO_3, acetone, room temperature, 12 h; (d) TFA/CH_2Cl_2 1:3, room temperature, overnight; (e) 1N NaOH, EtOH, reflux, 1 h; (f) zinc powder, acetic acid, room temperature,1 h.

and Figure 1) exhibited the highest inhibitory potency against DNMT1 and, when tested for its effects on the genome methylation levels in HL60 human myeloid leukemia cells, it revealed a recognizable demethylation of chromosomal satellite repeats.[55]

To extend structure−activity relationships for this class of inhibitors, we needed a scaffold more stable and versatile than the oxazoline ring. Therefore, we decided to explore the possibility of replacing it with the Δ^2-isoxazoline (**7a**−**k**) and to introduce a new conformational restriction (**8a**−**k**) as shown in Figure 1.

Herein we report the synthesis of such compounds and their inhibitory activity toward DNMT1 in both enzymatic and cellular assays. We also present the results of competition assays for the most potent enzyme inhibitor. These outcomes shed light into the binding site of the enzyme and served as basis to conduct molecular modeling studies of the inhibitor with a recently published crystallographic structure of human DNMT1.[75] To the best of our knowledge, this is the first molecular modeling study conducted with the crystallographic structure of human DNMT1.

CHEMISTRY

The key step for the synthesis of Δ^2-isoxazolines **7** was the 1,3-dipolar cycloaddition of nitrile oxides to allylic alcohol. Nitrile oxides were formed in situ by the corresponding aldoximes **9** after oxidative chlorination with aqueous NaOCl solution (common bleach), followed by base-induced dehydrochlorination of the intermediate hydroxymoyl chlorides (chlorooximes). The cycloaddition reaction afforded alcohols **10** in good isolated yields (93−68%) (Scheme 1).

The nucleophilic displacement of the corresponding mesylates **11** with dimethylamine furnished derivatives **7a**−**d**, **7h**−**j**, and **7l**. The carboxylic acid derivative **7e** was obtained by deprotecting the *t*-butyl ester **7l** with trifluoracetic acid at room temperature. The phenol derivative **7g** was obtained from the corresponding tosylate **7d** after hydrolysis with NaOH. Finally, reduction with zinc powder in acetic acid converted nitro derivatives **7b** and **7i** into the corresponding amino derivatives **7f** and **7k**, respectively.

Scheme 3. Synthesis of Aldoximes 9a−d, 9h−j, and 9l and chlorooximes 12a−d, 12h−j, and 12l[a]

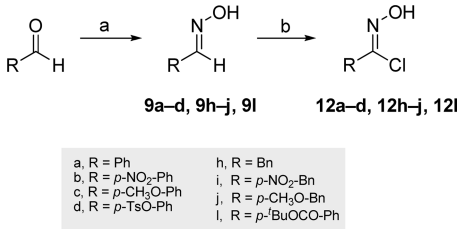

[a] Reagents and conditions: (a) $NH_2OH \cdot HCl$, Na_2CO_3, H_2O/methanol 1:1, room temperature, 3 h; (b) NCS, pyridine, $CHCl_3$, 40 °C, 0.5−3 h.

An analogous strategy was exploited to obtain bicyclic-Δ^2-isoxazolines **8** (Scheme 2). As previously reported by us,[76] *N*-Boc-protected pyrroline has low reactivity and the yields of 1,3-dipolar cycloaddition reaction are poor under conventional reaction conditions, even when the nitrile oxide is slowly generated from the corresponding stable chloroximes **12**. Conversely, running the reaction under continuous-flow conditions resulted in both an increased yield and an acceleration of the process, straightforwardly generating the *N*-Boc-protected bicyclic-Δ^2-isoxazolines **13**.[76]

Removal of the *N*-Boc group with 4 M HCl solution in dioxane and subsequent methylation with methyl iodide in acetone produced derivatives **8a**−**d**, **8h**−**j**, and **8l**. The carboxylic acid derivative **8e** was obtained by deprotecting the *t*-butyl ester **7l** with trifluoracetic acid at room temperature. Cleavage of the tosylate group of **8d** with NaOH in EtOH afforded derivative **8g**. Finally, reduction with zinc powder in acetic acid converted the nitro-substituted compounds **8b** and **8i** into the corresponding amino derivatives **8f** and **8k**, respectively.

The substituted oximes **9** were prepared from the corresponding aldehydes under standard conditions. Oximes **9** were then reacted with NCS in the presence of pyridine to give the corresponding chlorooximes **12a**−**d**, **12h**−**j**, and **12l** (Scheme 3).

dx.doi.org/10.1021/jm2010404 |*J. Med. Chem.* 2011, 54, 7663–7677

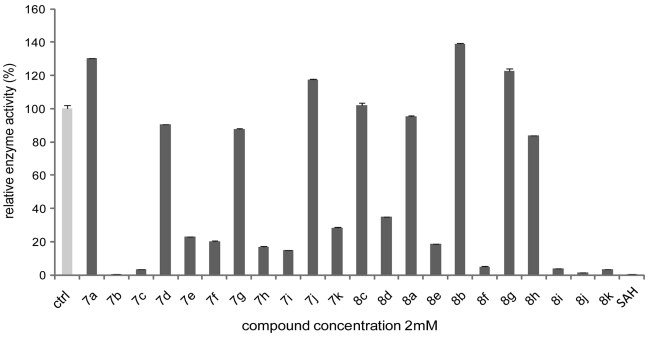

Figure 2. Biochemical DNMT activity assays for compounds **7a**−**k** and **8a**−**k** against recombinant human DNMT1. SAH was used as reference drug. All compounds were tested as 2 mM DMSO solutions. The assay sensitivity and the enzymatic activity required comparably high concentrations (500 nM) of enzyme and, consequently, high concentrations of test compounds. Error bars indicate standard deviations of each measurement. DMSO (2 mM) alone (ctrl) did not affect the enzymatic activity of DNMT1. Data are reported as mean ± SD of the relative enzyme activity in three independent experiments.

RESULTS AND DISCUSSION

Enzymatic Assays. So far, there is no standardized biochemical assay available that delivers reliable data of the enzymatic activity of DNMTs.[77] As previously reported,[53,55] we established a biochemical in vitro methylation assay using recombinant DNMT1 isolated and purified from insect cells. The identity and integrity of recombinant DNMT1 was confirmed by SDS gel electrophoresis and Western blotting with a DNMT1 specific antibody (data not shown). Enzymatic activity of purified DNMT1 was determined by the incorporation of radioactive labeled methyl groups into hemimethylated oligonucleotide substrates. Tritium labeled *S*-adenosylmethionine (SAM) was used as methyl group donor, and the incorporation of radioactivity was quantitated by a scintillation counter. The results showed that the recombinant DNMT1 enzyme has substantial enzymatic activity (Figure 2).

We performed a preliminary screening of the activity of compounds **7a**−**k** and **8a**−**k** at the single concentration of 2 mM, using procaine, **2**,[38,39] and *S*-adenosylhomocysteine (SAH) as reference compounds (2 mM DMSO solution). Procaine (as well as procainamide) was reported to inhibit DNMT activity at high drug concentrations. In addition, the assay sensitivity requires comparably high concentrations (500 nM) of enzyme and, consequently, high concentrations of test compounds. Even if accurate structure−activity relationships could not be derived from this assay, a few empirical considerations could be drawn pointing at the identification of potential inhibitors and to rule out inactive compounds.

It is noticeable that while both procaine and **2** were inactive in this assay, a number of tested compounds show a clear-cut inhibition of the enzyme activity (Figure 2 and Table 1), particularly when a nitro- or an amino- group is present as a substituent of the benzene ring (compounds **7b**, **7f**, **7i**, **7k** and **8b**, **8f**, **8i**, **8k**). Indeed, at the tested concentration, these compounds reduced the activity of DNMT1 at a very low level (0.3% in the case of **7b**, Table 1), a particularly significant outcome for non-nucleosidic inhibitors.

Similarly to what we previously reported for their oxazolino-analogues,[55] nitro-substituted isoxazolines derivatives seem to be more active than their amino- counterparts (nearly 70-fold in the case of compounds **7b** and **7f**, Table 1), but this become less evident (nearly 2-fold) when the phenyl ring linked to the heterocycles is replaced by a benzyl moiety (compare the inhibition elicited by compounds **7b** and **7f** with those elicited by **7i** and **7k**, respectively).

It is noteworthy that quite an opposite trend is observed in the case of bicyclic derivatives **8**. In fact, the nitrophenyl-substituted pyrrolidinoisoxazoline **8b** is 6-fold less active than its aminophenyl- counterpart (Table 1), whereas the activities of the benzylic analogues **8i** and **8k** are comparable. In a similar way, the introduction of the methoxy group produced active derivatives only in the case of phenyl-substituted isoxazolines (compound **7c**) and benzyl-substituted pyrrolidinoisoxazolines (compound **8j**), whereas the corresponding benzyl- and phenyl- analogues (compounds **7j** and **8c**, respectively) were inactive.

Table 1. Biochemical DNMT Assay of Compounds 7a−k and 8a−k against hDNMT1[a,b]

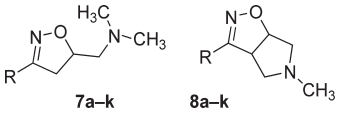

compd	R	mean (%)[a]	SD[b]
ctrl		100.3	1.78
7a	Ph	NA[c]	
7b	*p*-NO_2-Ph	0.3	0.02
7c	*p*-CH_3O-Ph	3.3	0.02
7d	*p*-TsO-Ph	90.6	0.09
7e	*p*-COOH-Ph	23.0	0.21
7f	*p*-NH_2-Ph	20.2	0.28
7g	*p*-OH-Ph	88.0	0.37
7h	Bn	17.1	0.08
7i	*p*-NO_2-−Bn	14.8	0.16
7j	*p*-CH_3O-Bn	NA[c]	
7k	*p*-NH_2-Bn	28.3	0.39
8a	Ph	NA[c]	
8b	*p*-NO_2-Ph	34.9	0.30
8c	*p*-CH_3O-Ph	95.6	0.39
8d	*p*-TsO-Ph	18.6	0.06
8e	*p*-COOH-Ph	NA[c]	
8f	*p*-NH_2-Ph	5.1	0.06
8g	*p*-OH-Ph	NA[c]	
8h	Bn	84.0	0.07
8i	*p*-NO_2-Bn	3.8	0.07
8j	*p*-CH_3O-Bn	1.7	0.02
8k	*p*-NH_2-Bn	3.3	0.05
procaine[d]		NA[c]	
2[d]		NA[c]	
SAH[d]		0.5	0.01

[a] The relative enzymatic activity (in percent) is shown as the mean value of three measurements. [b] Standard deviation values are indicated in percentage points. [c] Not active. [d] Procaine, RG108, and SAH (*S*-adenosylhomocysteine) were used as reference compounds. All compounds were tested in a concentration of 2 mM against 500 nM of DNMT1. Compounds with an inhibition greater than 20% were scored as positive.

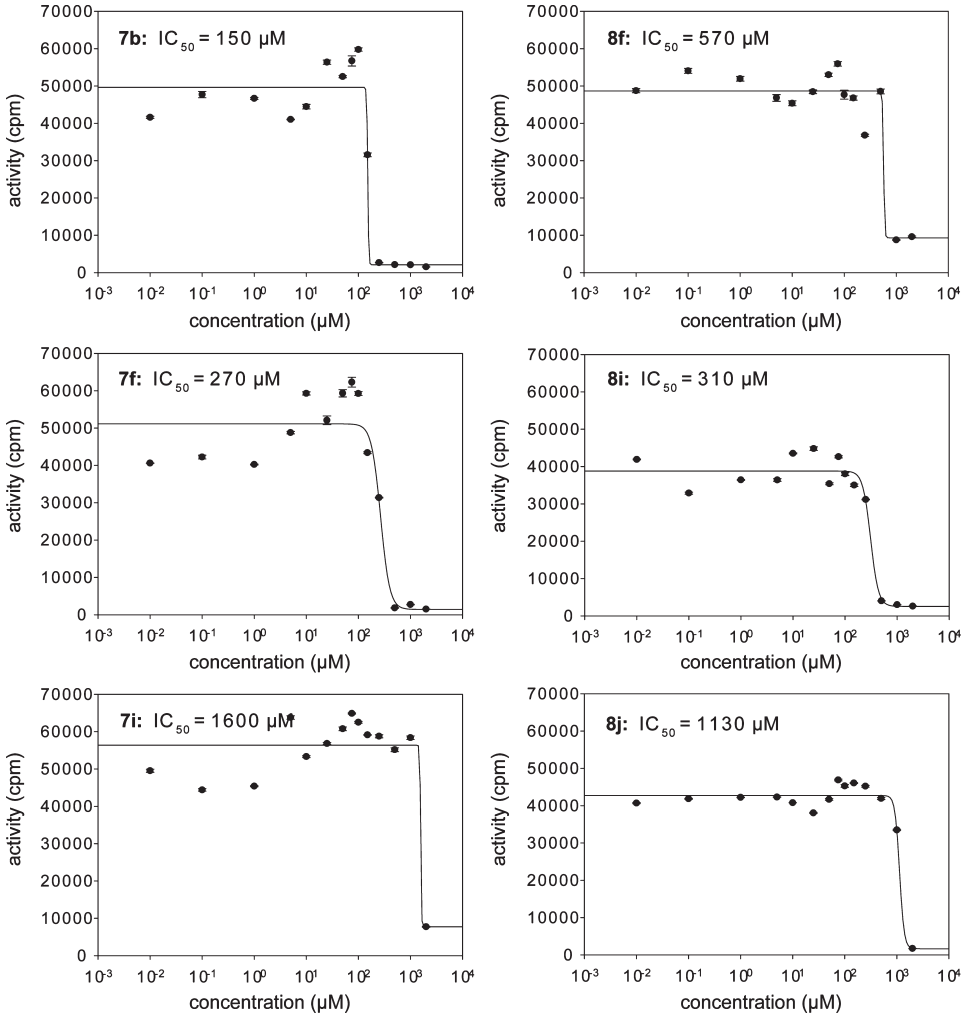

Figure 3. Dose−response plots for selected compounds **7b**, **7f**, **7i**, **8f**, **8i**, and **8j** against DNMT1. The IC_{50} concentrations of selected compounds were determined by biochemical DNMT assays under identical conditions (500 nM enzyme, 0.7 μM AdoMet, 400 nM hemimethylated oligo). Each data point represents the mean ± SD of three measurements, and the data were analyzed by SigmaPlot version 12.0.

Following the above considerations, we then selected derivatives **7b**, **7f**, **7i**, **8f**, **8i**, and **8j** among the most active compounds and carried out dose−response assay to generate curves from which the corresponding IC_{50} values were obtained (Figure 3). In agreement with results in Table 1, the nitrophenyl isoxazoline **7b** showed the highest inhibition of DNMT1 with an IC_{50} value of 150 μM, whereas its amino- counterpart **7f** as well as the aminophenyl- and the nitrobenzyl-substituted pyrrolidinoisoxazolines **8f** and **8i** were 2- to 4-fold less potent (IC_{50} values of 270, 570, and 310 μM, respectively). Both the nitrobenzyl isoxazolines **7i** and the methoxybenzyl pyrrolidinoisoxazoline **8j** were consistently less active (IC_{50} values of 1600 and 1130 μM, respectively). SAH was used as a nonspecific positive control and confirmed its efficient inhibition of DNMT1 (IC_{50} of 4 μM, dose−response curve not shown).

Competition Assays. As derivative **7b** emerged as the most promising candidate for further development, we decided to gain a better understanding of the kinetic mechanism(s) for the observed inhibition of DNMT1. Because mutational analyses are long-lasting and may affect the enzyme conformation, we applied a simple method reported by Lai and Wu for assessing the mode of inhibition.[78] According to this method, the mode of inhibition can be evaluated by holding the inhibitor constant at its IC_{50} concentration and varying the substrates. The behavior of the curves obtained under these conditions will point to the mode of inhibition. For DNMTs, these substrates are the methyl group donor SAM and the DNA (represented by a short oligo) and each of them binds to its distinct binding site in the catalytic domain of DNMT1. Therefore, the concentration of **7b** was kept constant at 150 μM (IC_{50} value, Figure 3), and either the SAM or the oligo substrate was varied (Figure 4). It can be seen that increasing the SAM concentration can nearly completely relieve the enzyme inhibition, whereas this is not affected by increasing the oligo substrate. According to the model,[78] this is consistent with an inhibitor that is competitive with respect to SAM and noncompetitive with respect to the oligo.

Inhibition of Cell Proliferation. Finally, we explored the effect of compound **7b** on the proliferation of HCT116 human colon carcinoma cell line. To this end, cells were incubated for 72 h with increasing concentrations (300, 500, and 750 μM) of **7b** in comparison to azacytidine (1 μM) or DMSO alone for control. The proliferation was assessed by counting viable cells after trypan blue staining. As shown in Figure 5, in these conditions compound **7b** induces a strong and dose-dependent antiproliferative effect,

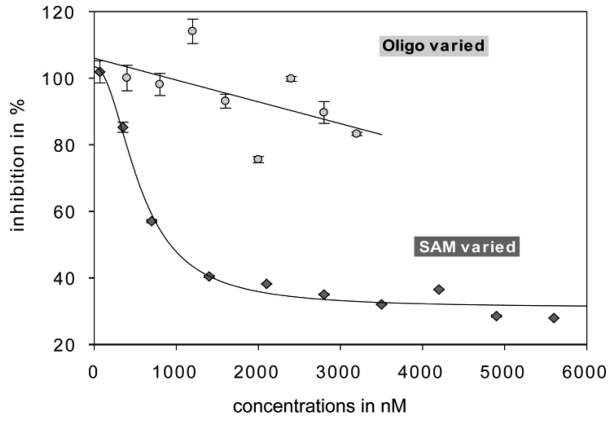

Figure 4. Derivative **7b** competes with the SAM binding site. The catalytic domain of DNMT1 has two binding sites, one for the oligo substrate and one for the SAM substrate. A modified biochemical DNMT activity assay was established to determine the mode of action of **7b**. Competition experiments were performed by increasing the concentration of the oligo substrate (oligo varied) or, alternatively, the SAM substrate (SAM varied). The assay was performed under standard conditions; please note that DNMT1 concentration was always kept constant (500 nM) as well as the inhibitor (**7b**) concentration (150 μM). The initial enzymatic activity under standard conditions in presence of the inhibitor was defined as 100% inhibition before increasing substrate concentrations to look for competition events. According to the model of Lai and Wu (see text), **7b** competes with SAM for the cofactor binding site but not for the oligo-binding site.

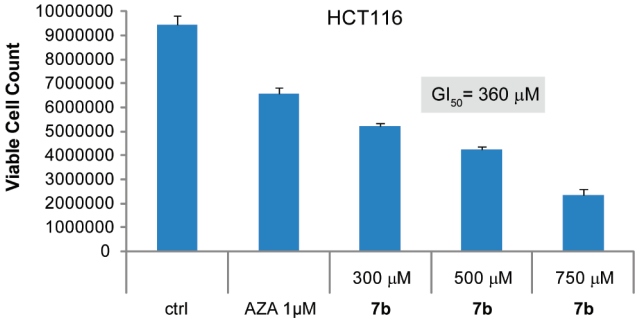

Figure 5. Derivative **7b** induces a strong antiproliferative effect after 72 h in HCT116 human colon carcinoma cells compared to DMSO treated cells. Azacytidine was included as a positive control. Ctrl are DMSO treated cells. GI_{50} value was determined by SigmaPlot 12.0.

with a GI_{50} value (the concentration of the compound that inhibits cell growth by 50%, calculated by SigmaPlot version 12.0, Systat Software Inc., San Jose, CA) of 360 μM. In the same assay, derivative **5b** does not affect the proliferation rate/doubling time (not shown).

Molecular Modeling Studies. On the basis of the results of the competition assay discussed above, the binding mode of **7b** into the binding pocket of the cofactor of human DNMT1 was analyzed using molecular modeling studies. Molecular docking and other computational approaches are increasingly being used to explore the ligand-binding interactions of DNMT inhibitors.[79−81] Until now, molecular modeling studies have been conducted using validated homology models of the methyltransferase domain of DNMT1.[79,80,82] However, a crystallographic structure of human DNMT1 has been recently published[75] which contains the methyltransferase domain bound

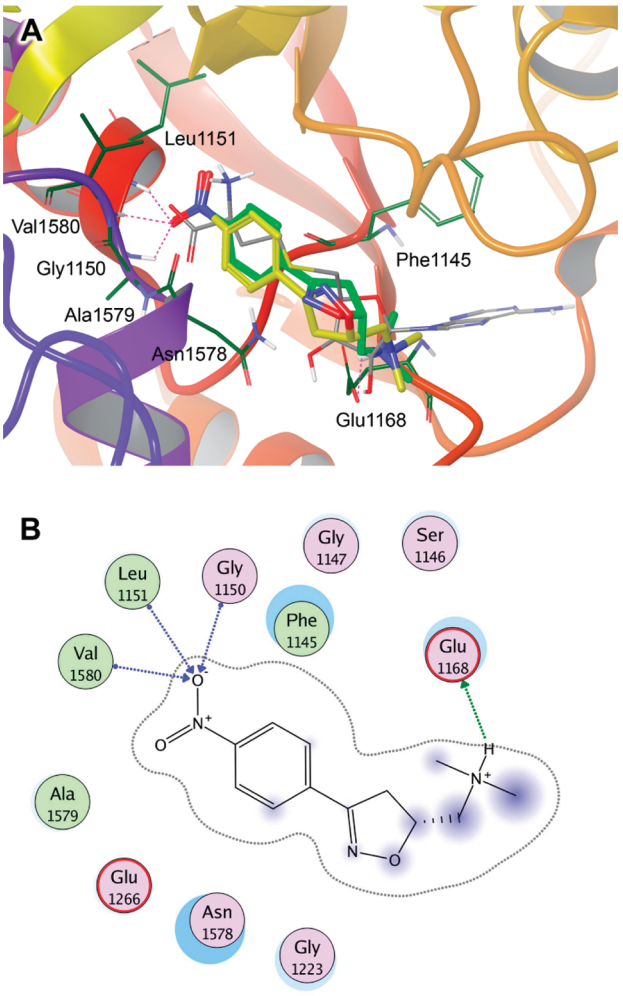

Figure 6. (A) Comparison of the binding modes of the *R* (green) and *S* (yellow) configurations of **7b** predicted by Glide. Crystallographic SAH (gray) is shown as reference. Hydrogen bonds for *R*-**7b** are displayed as magenta dashes. Selected amino acids residues within 4.5 Å of **7b** are shown. Nonpolar hydrogen atoms are omitted for clarity. (B) Two-dimensional interaction map displaying amino acid residues within 4.5 Å of *R*-**7b**. The ligand proximity contour is depicted with a dotted line. The ligand solvent exposure is represented with blue circles; larger and darker circles on ligand atoms indicate more solvent exposure. The receptor solvent exposure differences, in the presence and absence of the ligand, are represented by the size and intensity of the turquoise discs surrounding the residues; larger and darker discs indicate residues highly exposed to solvent in the active site when the ligand is absent. Figure created with the Ligand Interactions application of MOE.

to DNA-containing unmethylated CpG sites. On the basis of the experimental results of the competition assays, the binding of **7b** into the binding site of the cofactor was further explored using molecular docking. The docking protocol is presented in the Experimental Section. Briefly, the *R* and *S* configurations of **7b** in neutral and protonated forms (at the amino group) were flexibly docked into the crystallographic structure of the methyltransferase domain of human DNMT1 using Glide Extra Precision (XP), version 5.7.[83,84] Before docking **7b**, we tested the docking protocol for its ability to reproduce the experimental binding mode of the cocrystallized SAH.

To this end, SAH bound to the crystal structure was removed from the binding pocket and docked back into the cofactor

binding site. The root-mean-square deviation between the predicted conformation and the observed X-ray crystallographic conformation was 1.5 Å, indicating the capability of the docking protocol to reproduce the binding mode of SAH.

The calculated docking scores of the *R* and *S* configurations of **7b** in protonated form were −4.0 and −3.5 kcal/mol, respectively. The docking score of the neutral form of each configuration was −3.0 kcal/mol. These results suggest that **7b** binds to the cofactor binding site in the protonated form. The docking scores of **7b** were higher, i.e. less favorable, than the calculated docking score for SAH, which was −7.6 kcal/mol. The docking scores are in agreement with the results of the experimental DNMT1 inhibition assays, which shows that SAH is a more potent inhibitor than **7b** (see above).

Figure 6a shows a tridimensional binding model of the protonated *R* and *S* configurations (carbon atoms in green and yellow, respectively). The structure of cocrystallized SAH is shown as a reference (carbon atoms in gray).

As shown, Glide XP found a very similar binding mode for both *R* and *S* configurations. Together with the comparable docking energies calculated for the two configurations (see above), this hints that both enantiomers have similar enzymatic inhibitory activity. A two-dimensional representation of the binding mode of *R*-**7b** is shown in Figure 6b.

According to the derived docking model, **7b** occupies the binding site of the cofactor which is created by residues from the motifs I−III and X of the methyltransferase domain.[85] Compound **7b** binds in the region where the L-homocysteine and ribose moieties of SAH bind. The Δ^2-isoxazoline ring makes contacts with the side chain of Asn1578 and the backbone of Phe1145. The phenyl rings makes hydrophobic interactions mainly with Gly1147, Gly1223, Ala1579, and the backbone atoms of Ser1146 and Asn1578. The positively charged amino group forms a hydrogen bond with the side chain of Glu1168, which is located in motif II. Of note, two oxygen atoms (O2′ and O3′) of the ribose ring of SAH also form hydrogen bond interactions with the side chain of Glu1168. Similar hydrogen bond interactions with the equivalent glutamic acid residue are observed in other methyltransferases, e.g. Glu40 in the crystal structure of M.*Hha*I.[86]

The nitro group of **7b** occupies a region similar to the carboxylate group of SAH making similar interactions with the binding pocket. Hydrogen bonds between the oxygen atoms of the nitro group of **7b** and the backbone NH of Gly1150 (motif I), Leu1151, and Val1580 (motif X) were also predicted by Glide (Figure 6).[75,86]

CONCLUSION

The inactivation of tumor suppressor genes, which often results from epigenetic silencing associated with DNA hypermethylation, plays a pivotal role in the development of most forms of human cancer. Functional knockdown of DNMT1 is reported to reduce the genomic methylation patterns by approximately 93%.[87] Moreover, complete knock out of DNMT1 led to mitotic catastrophe in HCT116 cells,[88] indicating the interdependency of genomic methylation and cell viability but also substantiating the importance of targeting DNMT1 in cancer chemotherapy. Nucleoside analogues of cytosine (e.g., 5-azacytidine) effectively inhibit the activity of DNA methyltransferases, but their high cytotoxicity and the low therapeutic index make the development of novel non-nucleoside inhibitors highly desirable. Procaine and procainamide, already used as a local anesthetic and an antiarrhythmic drug, respectively, exhibit a weak DNA demethylating activity (even if at high drug concentrations) and are "repositionable" as non-nucleoside inhibitors. Following on our previous studies that led to the identification of a constrained analogue (**5b**) of procaine as a lead compound for the discovery of non-nucleoside inhibitors of DNMT1, we herein describe the preparation of a series of Δ^2-isoxazoline analogues (**7a**−**k** and **8a**−**k**) and their inhibitory activity toward DNMT1. While both procaine and **2** (see above) were inactive in this assay, a number of tested compounds show a clear inhibition of the enzyme activity. In particular, one of them, namely derivative **7b**, showed the highest inhibition of DNMT1 with an IC_{50} value of 150 μM, noteworthy nearly 10-fold improved compared to procaine or constrained analogue **5b**. Taking advantage of a simple method reported by Lai and Wu,[78] we assessed that the mode of inhibition of **7b** is consistent with a competition with the cofactor. Of note, these experiments represent one of the first efforts to elucidate experimentally the binding site of a non-nucleoside inhibitor of DNMT1. On the basis of the experimental evidence of the competition assays, we conducted molecular docking of **7b** into the binding site of the cofactor in order to explore its binding orientation and conformation. Docking simulations were conducted with the *R* and *S* configurations using the recently published crystallographic structure of the methyltransferase domain of human DNMT1.[75] To our knowledge, this is the first molecular modeling study reported with the crystallographic structure of human DNMT1. Both enantiomers showed comparable binding energy and a very similar binding mode. According to the binding model, compound **7b** binds in the same binding region of the L-homocysteine and ribose moieties of SAH and makes several hydrogen bonding interactions with amino acid residues common to SAH. Interestingly, these outcomes seem to exclude a direct interaction of **7b** with DNA, thus differentiating the mechanism of inhibition of this compound from those proposed for procaine[51] or procainamide.[52] As a matter of fact, whereas relatively high concentrations of these drugs are required for their inhibition of DNA methylation, derivative **7b** is far more potent in vitro (IC_{50} = 150 μM) and also exhibits a strong and dose-dependent antiproliferative effect against HCT116 human colon carcinoma cells. On the basis of these findings, we propose **7b** as a novel lead compound for the development of non-nucleoside DNMT inhibitors. As it competes with SAM for the binding site, a proper derivatization of this scaffold could lead to longer "bi-substrate" inhibitors, able to occupy both DNA and SAM binding pockets. Indeed, further studies are ongoing to develop analogues endowed with improved enzyme binding properties and higher inhibitory potency.

EXPERIMENTAL SECTION

Chemistry. All chemicals were purchased from Sigma Aldrich (Milan, Italy) or from Alfa Aesar GmbH (Karlsruhe, Germany) and were of the highest purity. All solvents were reagent grade and, when necessary, were purified and dried by standard methods. All reactions requiring anhydrous conditions were conducted under a positive atmosphere of nitrogen in oven-dried glassware. Standard syringe techniques were used for anhydrous addition of liquids. Reactions were routinely monitored by TLC performed on aluminum-backed silica gel plates (Merck DC, Alufolien Kieselgel 60 F254) with spots visualized by UV light (λ = 254, 365 nm) or using a $KMnO_4$ alkaline solution. Solvents were removed using a rotary evaporator operating at a reduced pressure of ~10 Torr. Organic solutions were dried over anhydrous Na_2SO_4. Chromatographic separations were

performed on silica gel (silica gel 60, 0.015−0.040 mm; Merck DC) columns. Melting points were determined on a Stuart SMP30 melting point apparatus in open capillary tubes and are uncorrected. ^{1}H NMR spectra were recorded at 300 MHz on a Bruker Avance 300 spectrometer. Chemical shifts are reported in δ (ppm) relative to the internal reference tetramethylsilane (TMS). When compounds were tested as salts, NMR data refer to the free base. Mass spectra were recorded on a Finnigan LCQ DECA TermoQuest (San Jose, USA) mass spectrometer in electrospray positive and negative ionization modes (ESI-MS). Purity of tested compounds was established by combustion analysis, confirming a purity ≥95%. Elemental analyses (C, H, N) were performed on a Perkin-Elmer 2400 CHN elemental analyzer at the laboratory of microanalysis of the Department of Chemistry and Biology, University of Salerno (Italy); the analytical results were within ±0.4% of the theoretical values. When the elemental analysis is not included, compounds were used in the next step without further purification.

General Procedure for Synthesis of Oximes (Compounds 9a−d, 9h−j, 9l). To a suspension of the proper aldehyde (30.0 mmol) and hydroxylamine hydrochloride (2.29 g, 33.0 mmol) in a 1:1 mixture of H_2O/methanol (40 mL), an aqueous solution of Na_2CO_3 (1.59 g, 15.0 mmol, 20 mL) was slowly added. The resulting mixture was stirred at room temperature for 3 h, and then methanol was evaporated. The aqueous phase was extracted with Et_2O (3 × 30 mL). The combined organic phases were washed with brine (30 mL), dried (Na_2SO_4), filtered, and concentrated in vacuo to give the title compounds **9**, which were used in the next step without further purification. Yields, physical, and spectral data of compounds are reported in Supporting Information.

General Procedure for Synthesis of Chlorooximes (Compounds 12a−d, 12h−j, 12l). To a solution of the proper aldoxime (2.75 mmol) in $CHCl_3$ (10 mL), pyridine was added (20 μL, 0.27 mmol). The reaction mixture was heated at 40 °C, and *N*-chlorosuccinimide (405 mg, 3.03 mmol) was added portionwise. After the reaction was complete (0.5−3 h, monitored by TLC), the mixture was diluted with CH_2Cl_2 (30 mL) and washed with brine (3 × 10 mL). The organic phase was dried (Na_2SO_4), filtered, and concentrated in vacuo to give the title compounds **12**, which were used in the cycloaddition step without further purification. Yields, physical, and spectral data of compounds are reported in Supporting Information.

General Procedure for Synthesis of 3-Substituted-5-hydroxymethyl-4,5-dihydroisoxazoles (Compounds 10a−d, 10h−j, 10l). To a vigorously stirred solution of the proper aldoxime (7.0 mmol) and allylic alcohol (0.81 mg, 0.95 mL, 14.0 mmol) in CH_2Cl_2 (50 mL) at 0 °C, a solution of common bleach (3% aqueous solution of NaOCl, 35 mL, 14.0 mmol) was added dropwise, keeping the temperature below 5 °C. The resulting biphasic mixture was vigorously stirred at room temperature for 15 min. The aqueous phase was separated and extracted with CH_2Cl_2 (3 × 20 mL). The combined organic phases were washed with brine (25 mL), dried (Na_2SO_4), filtered, and concentrated in vacuo. The residue was purified by silica gel chromatography (EtOAc/hexane) to give the title compounds **10**, which were recrystallized from the appropriate solvent.

*5-Hydroxymethyl-3-phenyl-4,5-dihydroisoxazole (**10a**).* White solid, 87% yield; mp (EtOAc/hexane) 83−84 °C. ^{1}H NMR (300 MHz, $CDCl_3$): δ 7.72−7.60 (m, 2H), 7.45−7.35 (m, 3H), 4.94−4.81 (m, 1H), 3.88 (ddd, *J* = 12.1, 6.3, 3.3 Hz, 1H), 3.68 (ddd, *J* = 12.1, 6.3, 4.7 Hz, 1H), 3.39 (dd, *J* = 16.5, 10.4 Hz, 1H), 3.29 (dd, *J* = 16.5, 8.0 Hz, 1H), 2.09 (t, *J* = 6.3 Hz, 1H). ESI-MS *m*/*z*: 178 (M + H)$^+$.

*5-Hydroxymethyl-3-(4-nitrophenyl)-4,5-dihydroisoxazole (**10b**).* Pale-yellow solid, 82%; mp (methanol) 141−143 °C. ^{1}H NMR (300 MHz, $CDCl_3$): δ 8.30 (d, *J* = 8.4 Hz, 2H), 7.84 (d, *J* = 8.4 Hz, 2H), 5.02−4.92 (m, 1H), 3.96 (ddd, *J* = 12.1, 4.4, 3.6 Hz, 1H), 3.72 (ddd, *J* = 12.1, 7.7, 4.4 Hz, 1H), 3.42 (dd, *J* = 16.5, 10.5, 1H), 3.36 (dd, *J* = 16.5, 8.5 Hz, 1H), 1.92−1.84 (m, 1H). ESI-MS *m*/*z*: 223 (M + H)$^+$.

*5-Hydroxymethyl-3-(4-methoxyphenyl)-4,5-dihydroisoxazole (**10c**).* White solid, 83% yield; mp (EtOAc) 144−146 °C. ^{1}H NMR (300 MHz, $CDCl_3$): δ 7.60 (d, *J* = 8.7 Hz, 2H), 6.92 (d, *J* = 8.7 Hz, 2H), 4.89−4.79 (m, 1H), 3.89−3.82 (m, 4H), 3.68 (dd, *J* = 12.0, 3.7 Hz, 1H), 3.37 (dd, *J* = 16.8, 10.7 Hz, 1H), 3.25 (dd, *J* = 16.8, 7.7 Hz, 1H), 1.80 (br s, 1H). ESI-MS *m*/*z*: 208 (M + H)$^+$.

*5-Hydroxymethyl-3-(4-(tosyloxy)phenyl)-4,5-dihydroisoxazole (**10d**).* White solid, 83% yield; mp (*i*-PrOH) 85−87 °C. ^{1}H NMR (300 MHz, $CDCl_3$): δ 7.68 (d, *J* = 8.0 Hz, 2H), 7.56 (d, *J* = 8.0 Hz, 2H), 7.30 (d, *J* = 8.0 Hz, 2H), 7.00 (d, *J* = 8.0 Hz, 2H), 4.90−4.79 (m, 1H), 3.84 (dd, *J* = 12.4, 3.3 Hz, 1H), 3.65 (dd, *J* = 12.4, 4.4 Hz, 1H), 3.32 (dd, *J* = 16.8, 11.0 Hz, 1H), 3.22 (dd, *J* = 16.8, 7.7 Hz, 1H), 2.43 (s, 3H), 2.18 (br s, 1H). ESI-MS *m*/*z*: 348 (M + H)$^+$.

*3-Benzyl-5-hydroxymethyl-4,5-dihydroisoxazole (**10h**).* Pale-yellow oil, 80% yield. ^{1}H NMR (300 MHz, $CDCl_3$): δ 7.40−7.15 (m, 5H), 4.70−4.58 (m, 1H), 3.71 (dd, *J* = 12.1, 3.3 Hz, 1H), 3.67 (s, 2H), 3.51 (dd, *J* = 12.1, 5.0 Hz, 1H), 2.85 (dd, *J* = 17.1, 10.5 Hz, 1H), 2.71 (dd, *J* = 17.1, 7.7 Hz, 1H), 2.10 (br s, 1H). ESI-MS *m*/*z*: 192 (M + H)$^+$.

*5-Hydroxymethyl-3-(4-nitrobenzyl)-4,5-dihydroisoxazole (**10i**).* Yellow solid, 93% yield; mp (EtOAc/hexane) 69−71 °C. ^{1}H NMR (300 MHz, $CDCl_3$): δ 8.20 (d, *J* = 8.5 Hz, 2H), 7.42 (d, *J* = 8.5 Hz, 2H), 4.74−4.66 (m, 1H), 3.89−3.70 (m, 3H), 3.53 (dd, *J* = 12.2, 4.1 Hz, 1H), 2.89 (dd, *J* = 17.6, 10.7 Hz, 1H), 2.79 (dd, *J* = 17.6, 7.5 Hz, 1H), 1.92 (br s, 1H). ESI-MS *m*/*z*: 237 (M + H)$^+$.

*5-Hydroxymethyl-3-(4-methoxybenzyl)-4,5-dihydroisoxazole (**10j**).* White solid, 78% yield; mp (isopropyl ether) 70−71 °C. ^{1}H NMR (300 MHz, $CDCl_3$): δ 7.11 (d, *J* = 8.5 Hz, 2H), 6.82 (d, *J* = 8.5 Hz, 2H), 4.66−4.54 (m, 1H), 3.76 (s, 3H), 3.66 (dd, *J* = 12.3, 3.2 Hz, 1H), 3.58 (s, 2H), 3.48 (dd, *J* = 12.3, 4.6 Hz, 1H), 2.82 (dd, *J* = 17.3, 11.0 Hz, 1H), 2.68 (dd, *J* = 17.3, 7.8. Hz, 1H), 2.58 (br s, 1H). ESI-MS *m*/*z*: 222 (M + H)$^+$.

*3-(4-tert-Butyloxycarbonylphenyl)-5-hydroxymethyl-4,5-dihydroisoxazole (**10l**).* White solid, 68% yield; mp (*i*-PrOH) 89−91 °C. ^{1}H NMR (300 MHz, $CDCl_3$): δ 7.99 (d, *J* = 8.8 Hz, 2H), 7.69 (d, *J* = 8.8 Hz, 2H), 4.96−4.84 (m, 1H), 3.90 (dd, *J* = 12.4, 3.0 Hz, 1H), 3.70 (dd, *J* = 12.4, 4.1 Hz, 1H), 3.40 (dd, *J* = 16.8, 10.7 Hz, 1H), 3.30 (dd, *J* = 16.8, 8.2 Hz, 1H), 2.20 (br s, 1H), 1.60 (s, 9H). ESI-MS *m*/*z*: 278 (M + H)$^+$.

General Procedure for Synthesis of (3-Substituted-4,5-dihydroisoxazol-5-yl)methyl Methanesulfonate (Compounds 11a−d, 11h−j, 11l). To a solution of the proper (3-substituted-4,5-dihydroisoxazol-5-yl)methanol **10** (1.66 mmol) and triethylamine (0.28 mL, 2.00 mmol) in dry CH_2Cl_2 (20 mL), methanesulfonyl chloride (0.16 mL, 2.00 mmol) was added at 0 °C. The resulting mixture was stirred at room temperature for 45 min, and then the solvent was evaporated. The residue was taken up with water (20 mL) and extracted with CH_2Cl_2 (3 × 20 mL). The combined organic phases were washed with 1N HCl (2 × 10 mL), $NaHCO_3$, saturated aqueous solution (2 × 10 mL), and brine (10 mL), dried (Na_2SO_4), filtered, and concentrated in vacuo. Mesylates **11** were obtained in quantitative yields and used without further purification in the subsequent reaction. Recrystallization from the suitable solvent gave an analytical sample.

*5-Hydroxymethyl-3-phenyl-4,5-dihydroisoxazole Methanesulfonate (**11a**).* White solid; mp (*i*-PrOH) 109−111 °C. ^{1}H NMR (300 MHz, $CDCl_3$): δ 7.70−7.60 (m, 2H), 7.42−7.38 (m, 3H), 5.06−4.96 (m, 1H), 4.39 (dd, *J* = 11.3, 3.9 Hz, 1H), 4.27 (dd, *J* = 11.3, 5.0 Hz, 1H), 3.45 (dd, *J* = 17.0, 11.0 Hz, 1H), 3.30 (dd, *J* = 17.0, 7.2 Hz, 1H), 3.09 (s, 3H). ESI-MS *m*/*z*: 256 (M + H)$^+$.

*5-Hydroxymethyl-3-(4-nitrophenyl)-4,5-dihydroisoxazole Methanesulfonate (**11b**).* White solid; mp: (MeOH/H_2O) 171−173 °C. ^{1}H NMR (300 MHz, $CDCl_3$): δ 8.29 (d, *J* = 8.8 Hz, 2H), 7.84 (d, *J* = 8.8 Hz, 2H), 5.19−5.06 (m, 1H), 4.45 (dd, *J* = 11.3, 4.1 Hz, 1H), 4.39 (dd, *J* = 11.3, 4.7 Hz, 1H), 3.54 (dd, *J* = 16.8, 11.0 Hz, 1H), 3.36 (dd, *J* = 16.8, 7.2 Hz, 1H), 3.09 (s, 3H). ESI-MS *m*/*z*: 301 (M + H)$^+$.

*5-Hydroxymethyl-3-(4-methoxyphenyl)-4,5-dihydroisoxazole Methanesulfonate (**11c**).* White solid; mp: (EtOAc) 146−148 °C. ^{1}H NMR

(300 MHz, $CDCl_3$): δ 7.60 (d, J = 8.8 Hz, 2H), 6.93 (d, J = 8.8 Hz, 2H), 5.04−4.94 (m, 1H), 4.40 (dd, J = 11.3, 4.1 Hz, 1H), 4.34 (dd, J = 11.3, 5.0 Hz, 1H), 3.85 (s, 3H), 3.48 (dd, J = 16.8, 11.0 Hz, 1H), 3.28 (dd, J = 16.8, 7.2 Hz, 1H), 3.09 (s, 3H). ESI-MS *m/z*: 286 $(M + H)^+$.

*5-Hydroxymethyl-3-(4-(tosyloxy)phenyl)-4,5-dihydroisoxazole Methanesulfonate (**11d**).* White solid; mp: (*i*-PrOH) 123−125 °C. ^1H NMR (300 MHz, $CDCl_3$): δ 7.69 (d, J = 8.5 Hz, 2H), 7.57 (d, J = 8.5 Hz, 2H), 7.32 (d, J = 8.5 Hz, 2H), 7.02 (d, J = 8.5 Hz, 2H), 5.07−4.95 (m, 1H), 4.38 (dd, J = 11.6, 3.9 Hz, 1H), 4.31 (dd, J = 11.6, 3.9 Hz, 1H), 3.44 (dd, J = 17.1, 11.0 Hz, 1H), 3.24 (dd, J = 17.1, 7.1 Hz, 1H), 3.06 (s, 3H), 2.44 (s, 3H). ESI-MS *m/z*: 426 $(M + H)^+$.

*3-Benzyl-5-hydroxymethyl-4,5-dihydroisoxazole Methanesulfonate (**11h**).* White solid; mp (*i*-PrOH): 43−44 °C. ^1H NMR (300 MHz, $CDCl_3$): δ 7.38−7.20 (m, 5H), 4.82−4.72 (m, 1H), 4.22 (dd, J = 11.3, 3.9 Hz, 1H), 4.15 (dd, J = 11.3, 5.0 Hz, 1H), 3.66 (s, 2H), 2.98 (s, 3H), 2.96 (dd, J = 17.6, 10.9 Hz, 1H), 2.71 (dd, J = 17.6, 7.0 Hz, 1H). ESI-MS *m/z*: 270 $(M + H)^+$.

*5-Hydroxymethyl-3-(4-nitrobenzyl)-4,5-dihydroisoxazole Methanesulfonate (**11i**).* Pale-yellow solid; mp (*i*-PrOH): 107−109 °C. ^1H NMR (300 MHz, $CDCl_3$): δ 8.24 (d, J = 8.8 Hz, 2H), 7.45 (d, J = 8.8 Hz, 2H), 4.92−4.81 (m, 1H), 4.29 (dd, J = 11.3, 3.8 Hz, 1H), 4.21 (dd, J = 11.3, 4.4 Hz, 1H), 3.83 (s, 2H), 3.08 (s, 3H), 3.02 (dd, J = 17.4, 10.8 Hz, 1H). 2.82 (dd, J = 17.4, 6.8 Hz, 1H). ESI-MS *m/z*: 315 $(M + H)^+$.

*5-Hydroxymethyl-3-(4-methoxybenzyl)-4,5-dihydroisoxazole Methanesulfonate (**11j**).* White solid; mp (*i*-PrOH): 104−105 °C. ^1H NMR (300 MHz, $CDCl_3$): δ 7.12 (d, J = 8.7 Hz, 2H), 6.83 (d, J = 8.7 Hz, 2H), 4.83−4.72 (m, 1H), 4.24 (dd, J = 11.3, 3.9 Hz, 1H), 4.17 (dd, J = 11.3, 5.0 Hz, 1H), 3.79 (s, 3H), 3.62 (s, 2H), 3.03 (s, 3H), 2.96 (dd, J = 17.3, 11.0 Hz, 1H), 2.72 (dd, J = 17.3, 7.1 Hz, 1H). ESI-MS *m/z*: 300 $(M + H)^+$.

*3-(4-tert-Butyloxycarbonylphenyl)-5-hydroxymethyl-4,5-dihydroisoxazole Methanesulfonate (**11l**).* White solid; mp (*i*-PrOH): 128−129 °C. ^1H NMR (300 MHz, $CDCl_3$): δ 8.02 (d, J = 8.8 Hz, 2H), 7.68 (d, J = 8.8 Hz, 2H), 5.12−4.99 (m, 1H), 4.42 (dd, J = 11.7, 4.1 Hz, 1H), 4.35 (dd, J = 11.7, 5.0 Hz, 1H), 3.52 (dd, J = 17.0, 11.1 Hz, 1H), 3.30 (dd, J = 17.0, 7.3 Hz, 1H), 3.08 (s, 3H), 1.60 (s, 9H). ESI-MS *m/z*: 356 $(M + H)^+$.

General Procedure for Synthesis of 3-Substituted-5-(*N*,*N*-dimethylaminomethyl)-4,5-dihydroisoxazoles (Compounds 7a−d, 7h−j, 7l). The proper mesylate (1.30 mmol) was dissolved in a 2 M THF solution of dimethylamine (20 mL, 39.0 mmol) under N_2 atmosphere. The vessel was sealed, and the reaction was stirred at 100 °C for 12 h and then concentrated in vacuo. The residue was purified by silica gel chromatography (EtOAc/hexane) to give the title compounds. Compounds **7c,d** and **7l** were recrystallized from the appropriate solvent. Compounds **7a,b**, and **7h−j** were dissolved in 4N HCl in dioxane, and the mixture was stirred at room temperature for 10 min. The solvent was concentrated in vacuo, and the resulting solid was recrystallized from the appropriate solvent to yield title compounds as hydrochloride salts.

*5-(N,N-Dimethylaminomethyl)-3-phenyl-4,5-dihydroisoxazole Hydrochloride (**7a**).* White solid, 79% yield; mp (2-propanol) 188−190 °C; free base. ^1H NMR (300 MHz, $CDCl_3$): δ 7.62−7.51 (m, 2H), 7.35−7.23 (m, 3H), 4.86−4.72 (m, 1H), 3.30 (dd, J = 16.5, 10.5 Hz, 1H), 3.05 (dd, J = 16.5, 8.0 Hz, 1H), 2.53 (dd, J = 12.7, 6.6 Hz, 1H), 2.46 (dd, J = 12.7, 5.2 Hz, 1H), 2.24 (s, 6H). ESI-MS *m/z*: 205 $(M + H)^+$. Anal. ($C_{12}H_{16}N_2O \cdot HCl$) C, H, N.

*5-(N,N-Dimethylaminomethyl)-3-(4-nitrophenyl)-4,5-dihydroisoxazole Hydrochloride (**7b**).* White solid, 78% yield; mp (methanol) 262 °C (decomp); free base. ^1H NMR (300 MHz, $CDCl_3$): δ 8.26 (d, J = 8.7 Hz, 2H), 7.84 (d, J = 8.7 Hz, 2H), 5.06−4.90 (m, 1H), 3.43 (dd, J = 16.7, 10.6 Hz, 1H), 3.24 (dd, J = 16.7, 8.1 Hz, 1H), 2.66 (dd, J = 12.8, 6.4 Hz, 1H), 2.55 (dd, J = 12.8, 6.0 Hz, 1H), 2.34 (s, 6H). ESI-MS *m/z*: 250 $(M + H)^+$. Anal. ($C_{12}H_{15}N_3O_3 \cdot HCl$) C, H, N.

*5-(N,N-Dimethylaminomethyl)-3-(4-methoxyphenyl)-4,5-dihydroisoxazole (**7c**).* White solid, 75% yield; mp (diisopropylether) 75−76 °C. ^1H NMR (300 MHz, $CDCl_3$): δ 7.61 (d, J = 8.8 Hz, 2H), 6.91 (d, J = 8.8 Hz, 2H), 4.93−4.80 (m, 1H), 3.83 (s, 3H), 3.40 (dd, J = 16.7, 10.5 Hz, 1H), 3.14 (dd, J = 16.7, 7.6 Hz, 1H), 2.63 (dd, J = 12.9, 6.7 Hz, 1H), 2.55 (dd, J = 12.9, 5.6 Hz, 1H), 2.35 (s, 6H). ESI-MS *m/z*: 235 $(M + H)^+$. Anal. ($C_{13}H_{18}N_2O_2$) C, H, N.

*5-(N,N-Dimethylaminomethyl)-3-(4-(tosyloxy)phenyl)-4,5-dihydroisoxazole (**7d**).* White solid, 78% yield; mp (2-propanol) 123−124 °C. ^1H NMR (300 MHz, $CDCl_3$): δ 7.70 (d, J = 8.2 Hz, 2H), 7.57 (d, J = 8.2 Hz, 2H), 7.31 (d, J = 8.2 Hz, 2H), 7.00 (d, J = 8.2 Hz, 2H), 4.93−4.82 (m, 1H), 3.32 (dd, J = 16.8, 10.5 Hz, 1H), 3.12 (dd, J = 16.8, 8.0 Hz, 1H), 2.60 (dd, J = 12.9, 6.3 Hz, 1H), 2.49 (dd, J = 12.9, 6.3 Hz, 1H), 2.43 (s, 3H), 2.31 (s, 6H). ESI-MS *m/z*: 375 $(M + H)^+$. Anal. ($C_{19}H_{22}N_2O_4S$) C, H, N.

*3-Benzyl-5-(N,N-dimethyl-aminomethyl)-4,5-dihydroisoxazole Hydrochloride (**7h**).* White solid, 76% yield; mp (EtOAc) 80−82 °C; free base. ^1H NMR (300 MHz, $CDCl_3$): δ 7.35−7.22 (m, 5H), 4.70−4.60 (m, 1H), 3.68 (s, 2H), 2.86 (dd, J = 17.0, 10.4 Hz, 1H), 2.60 (dd, J = 17.0, 8.0 Hz, 1H), 2.50 (dd, J = 12.8, 6.5 Hz, 1H), 2.33 (dd, J = 12.8, 5.7 Hz, 1H), 2.25 (s, 6H). ESI-MS *m/z*: 219 $(M + H)^+$. Anal. ($C_{13}H_{18}N_2O \cdot HCl$) C, H, N.

*5-(N,N-Dimethyl-aminomethyl)-3-(4-nitrobenzyl)-4,5-dihydroisoxazole Hydrochloride (**7i**).* White solid, 79% yield; mp (EtOH/Et_2O) 164−167 °C; free base. ^1H NMR (300 MHz, $CDCl_3$): δ 8.20 (d, J = 8.8 Hz, 2H), 7.42 (d, J = 8.8 Hz, 2H), 4.78−4.66 (m, 1H), 3.78 (s, 2H), 2.89 (dd, J = 17.0, 10.4 Hz, 1H), 2.65 (dd, J = 17.0, 8.0 Hz, 1H), 2.52 (dd, J = 12.9, 6.5 Hz, 1H), 2.40 (dd, J = 12.9, 5.5 Hz, 1H), 2.27 (s, 6H). ESI-MS *m/z*: 264 $(M + H)^+$. Anal. ($C_{13}H_{17}N_3O_3 \cdot HCl$) C, H, N.

*5-(N,N-Dimethylaminomethyl)-3-(4-methoxybenzyl)-4,5-dihydroisoxazole Hydrochloride (**7j**).* White solid, 79% yield; mp (acetone/Et_2O) 126−128 °C; free base. ^1H NMR (300 MHz, $CDCl_3$): δ 7.14 (d, J = 8.5 Hz, 2H), 6.86 (d, J = 8.5 Hz, 2H), 4.69−4.59 (m, 1H), 3.79 (s, 3H), 3.61 (s, 2H), 2.86 (dd, J = 16.9, 10.3 Hz, 1H), 2.59 (dd, J = 16.9, 8.0 Hz, 1H), 2.49 (dd, J = 12.8, 6.6 Hz, 1H), 2.33 (dd, J = 12.8, 5.7 Hz, 1H), 2.25 (s, 6H). ESI-MS *m/z*: 249 $(M + H)^+$. Anal. ($C_{14}H_{20}N_2O_2 \cdot HCl$) C, H, N.

*5-(N,N-Dimethylaminomethyl)-3-(4-tert-butyloxycarbonylphenyl)-4,5-dihydroisoxazole (**7l**).* White solid, 81% yield; mp (*i*-PrOH) 75−76 °C. ^1H NMR (300 MHz, $CDCl_3$): δ 8.00 (d, J = 8.8 Hz, 2H), 7.70 (d, J = 8.8 Hz, 2H), 4.98−4.84 (m, 1H), 3.41 (dd, J = 16.7, 10.6 Hz, 1H), 3.18 (dd, J = 16.7, 8.2 Hz, 1H), 2.63 (dd, J = 12.9, 6.2 Hz, 1H), 2.52 (dd, J = 12.9, 6.2 Hz, 1H), 2.32 (s, 6H), 1.60 (s, 9H). ESI-MS *m/z*: 305 $(M + H)^+$.

Synthesis of 5-(*N*,*N*-Dimethylaminomethyl)-3-(4-hydroxyphenyl)-4,5-dihydroisoxazole Hydrochloride (7g). To a solution of **7d** (110 mg, 0.29 mmol) in EtOH (5 mL) an aqueous solution of 1N NaOH (1.45 mL, 1.45 mmol) was added. The mixture was heated at reflux and stirred for 1 h. The reaction mixture was then cooled to room temperature, treated with HCl 1 N to pH 9, and concentrated in vacuo. The residue was treated with water (30 mL) and extracted with EtOAc (3 × 30 mL). The combined organic phases were washed with brine (10 mL), dried (Na_2SO_4), filtered, and concentrated in vacuo to give the title compound as a free base (61.2 mg, 96%), which was converted in the corresponding hydrochloride salt following the general procedure described for compounds **7a,b**, and **7h−j**; mp 232−235 °C (decomp); free base. ^1H NMR (300 MHz, DMSO-d_6): δ 9.90 (br s, 1H), 7.47 (d, J = 8.5 Hz, 2H), 6.80 (d, J = 8.5 Hz, 2H), 4.77−4.66 (m, 1H), 3.37 (dd, J = 16.9, 11.7 Hz, 1H), 3.07 (dd, J = 16.9, 8.0 Hz, 1H), 2.51−2.39 (m, 2H), 2.20 (s, 6H). ESI-MS *m/z*: 221 $(M + H)^+$. Anal. ($C_{12}H_{16}N_2O_2 \cdot HCl$) C, H, N.

Synthesis of 5-(*N*,*N*-Dimethylaminomethyl)-3-(4-carboxyphenyl)-4,5-dihydroisoxazole (7e). A mixture of TFA and DCM (1:3, 12 mL) was added to compound **7l** (314 mg, 1.03 mmol). The reaction was stirred at room temperature overnight and then concentrated in vacuo to give the title compound as a white solid (256 mg, 99%), which was recrystallized from methanol/H_2O. White solid; mp 249−251 °C (decomp). ^1H NMR (300 MHz, DMSO-d_6): δ 9.96 (br s, 1H), 8.0 (d, J = 8.2 Hz, 2H), 7.78 (d, J = 8.2 Hz, 2H), 5.25−5.15 (m,

1H), 3.80−3.63 (m, 1H), 3.50−3.23 (m, 3H), 2.84 (s, 6H). ESI-MS *m/z*: 249 $(M + H)^+$. Anal. ($C_{13}H_{16}N_2O_3$) C, H, N.

Synthesis of 5-(*N*,*N*-Dimethylaminomethyl)-3-(4-amminophenyl)-4,5-dihydroisoxazole Hydrochloride (7f). To an ice cooled solution of **7b** free base (160 mg, 0.64 mmol) in AcOH (36 mL) zinc powder (336 mg, 5.13 mmol) was added. The resulting mixture was stirred at room temperature for 1 h, the solid was filtered off, and the solvent was evaporated. The residue was taken up with EtOAc (20 mL) and washed with $NaHCO_3$ saturated aqueous solution twice. The organic phase was dried (Na_2SO_4), filtered, and concentrated in vacuo. The residue was purified by silica gel chromatography (CH_2Cl_2/MeOH) to give the title compound (121 mg, 63%), which was converted in the corresponding hydrochloride salt following the general procedure described for compounds **7a,b**, and **7h−j**. White solid; mp 268−270 °C (decomp); free base. ^{1}H NMR (300 MHz, $CDCl_3$): δ 7.47 (d, J = 8.8 Hz, 2H), 6.67 (d, J = 8.8 Hz, 2H), 4.86−4.76 (m, 1H), 3.87 (br s, 2H); 3.36 (dd, J = 16.5, 10.3 Hz, 1H), 3.11 (dd, J = 16.5, 7.8 Hz, 1H), 2.60 (dd, J = 12.8, 6.4 Hz, 1H), 2.50 (dd, J = 12.8, 6.1 Hz, 1H), 2.32 (s, 6H). ESI-MS *m/z*: 220 $(M + H)^+$. Anal. ($C_{12}H_{17}N_3O\cdot HCl$) C, H, N.

5-(*N*,*N*-Dimethylaminomethyl)-3-(4-aminobenzyl)-4,5-dihydroisoxazole Hydrochloride (7k). Reduction of compound **7i** (154 mg, 0.58 mmol) according to the procedure used for **7f** yielded the free amine (102 mg, 75%), which was converted to the hydrochloride salt following the general procedure described for compounds **7a,b**, and **7h−j**. White solid; mp (EtOH/Et_2O) 211−212 °C (decomp); free base. ^{1}H NMR (300 MHz, $CDCl_3$): δ 6.99 (d, J = 8.2 Hz, 2H), 6.62 (d, J = 8.2 Hz, 2H), 4.79−4.46 (m, 1H), 3.75 (br s, 2H), 3.54 (s, 2H), 2.86 (dd, J = 17.0, 10.3 Hz, 1H), 2.58 (dd, J = 17.0, 10.3 Hz, 1H), 2.50 (dd, J = 12.8, 7.0 Hz, 1H), 2.35 (dd, J = 12.8, 5.5 Hz, 1H), 2.26 (s, 6H). ESI-MS *m/z*: 234 $(M + H)^+$. Anal. ($C_{13}H_{19}N_3O\cdot HCl$) C, H, N.

General Procedure for the Synthesis of *tert*-Butyl 3-Substituted-6,6a-dihydro-3a*H*-pyrrolo[3,4-*d*]isoxazole-5(4*H*)-carboxylates (Compounds 13a−d, 13h−j, 13l). A 0.25 M solution of *N*-Boc-3-pyrroline **9** (169 mg, 1.00 mmol) in EtOAc (4 mL) and a 0.37 M solution of the proper chloroxime **12** (1.50 mmol) in EtOAc (4 mL) were prepared. The two reactant streams were mixed using a simple T-piece and delivered to an Omnifit glass column (6.6 mm id by 100 mm length) filled with K_2CO_3 (540 mg, 4.00 mmol) heated at 90 °C at a total flow rate of 0.1 mL min^{-1}, equivalent to a residence time of about 10 min. A 100 psi backpressure regulator was applied to the system. The solvent was evaporated, and the product was purified by silica gel column chromatography (hexane/EtOAc 7:3) to give the title compound **13**.

*tert-Butyl 3-Phenyl-6,6a-dihydro-3aH-pyrrolo[3,4-d]isoxazole-5(4H)-carboxylate (**13a**)*[76]. White solid, 69% yield; mp (EtOAc/hexane) 146−147 °C (decomp). ^{1}H NMR (300 MHz, $CDCl_3$): δ 7.65−7.55 (m, 2H), 7.45−7.35 (m, 3H), 5.28 (ddd, J = 9.3, 5.5, 1.1 Hz, 1H), 4.25−4.15 (m, 1H), 3.90 (d, J = 12.6 Hz, 1H), 3.51−3.70 (m, 3H), 1.40 (s, 9H). ESI-MS *m/z*: 233 $(M + H - {}^tBu)^+$.

*tert-Butyl 3-(4-Nitrophenyl)-6,6a-dihydro-3aH-pyrrolo[3,4-d]isoxazole-5(4H)-carboxylate (**13b**)*[76]. Pale-yellow solid, 60% yield; mp (EtOAc/hexane) 189−190 °C (decomp). ^{1}H NMR (300 MHz, $CDCl_3$): δ 8.28 (d, J = 8.8 Hz, 2H), 7.80 (d, J = 8.8 Hz, 2H), 5.40 (dd, J = 8.3, 4.1 Hz, 1H), 4.30−4.20 (m, 1H), 4.03 (d, J = 13.2 Hz, 1H), 3.85−3.55 (m, 3H), 1.42 (s, 9H). ESI-MS *m/z*: 278 $(M + H - {}^tBu)^+$.

*tert-Butyl 3-(4-Methoxyphenyl)-6,6a-dihydro-3aH-pyrrolo[3,4-d]isoxazole-5(4H)-carboxylate (**13c**)*[76]. White solid, 73% yield; mp (EtOAc/hexane) 137−138 °C. ^{1}H NMR (300 MHz, $CDCl_3$): δ 7.56 (d, J = 8.8 Hz, 2H), 6.93 (d, J = 8.8 Hz, 2H), 5.26 (dd, J = 9.3, 5.2 Hz, 1H), 4.25−4.15 (m, 1H), 3.95 (d, J = 12.6 Hz, 1H), 3.83 (s, 3H), 3.72−3.58 (m, 3H), 1.40 (s, 9H). ESI-MS *m/z*: 263 $(M + H - {}^tBu)^+$.

*tert-Butyl 3-(4-(Tosyloxy)phenyl)-6,6a-dihydro-3aH-pyrrolo[3,4-d]isoxazole-5(4H)-carboxylate (**13d**)*[76]. Pale-yellow solid, 58% yield; mp (EtOAc/hexane) 189−190 °C. ^{1}H NMR (300 MHz, $CDCl_3$): δ 7.72 (d, J = 8.2 Hz, 2H), 7.56 (d, J = 8.2 Hz, 2H), 7.33 (d, J = 7.8 Hz, 2H), 7.04 (d, J = 7.8 Hz, 2H), 5.34 (dd, J = 9.5, 5.1 Hz, 1H), 4.25−4.13 (m, 1H), 4.00 (d, J = 12.9 Hz, 1H), 3.85−3.55 (m, 3H), 2.46 (s, 3H), 1.42 (s, 9H). ESI-MS *m/z*: 403 $(M + H - {}^tBu)^+$.

*tert-Butyl 3-Benzyl-6,6a-dihydro-3aH-pyrrolo[3,4-d]isoxazole-5(4H)-carboxylate (**13h**)*[76]. Pale-yellow oil, 71% yield. ^{1}H NMR (300 MHz, $CDCl_3$): δ 7.21−7.37 (m, 5H), 5.08 (ddd, J = 9.1, 5.6, 1.5 Hz, 1H), 3.95−3.80 (m, 3H), 3.62−3.50 (m, 2H), 3.45 (dd, J = 13.5, 5.6 Hz, 1H), 3.29 (dd, J = 11.7, 8.5 Hz, 1H), 1.45 (s, 9H). ESI-MS *m/z*: 325 $(M + Na)^+$.

*tert-Butyl 3-(4-Nitrobenzyl)-6,6a-dihydro-3aH-pyrrolo[3,4-d]isoxazole-5(4H)-carboxylate (**13i**)*[76]. Yellow solid, 67% yield; mp (EtOAc/hexane) 108−110 °C. ^{1}H NMR (300 MHz, $CDCl_3$): δ 8.20 (d, J = 8.5 Hz, 2H), 7.45 (d, J = 8.5 Hz, 2H), 5.12 (dd, J = 8.2, 4.8 Hz, 1H), 4.00−3.80 (m, 2H), 3.75−3.55 (m, 3H), 3.45 (dd, J = 12.6, 4.8 Hz, 1H), 3.32 (dd, J = 11.8, 8.2 Hz, 1H), 1.42 (s, 9H). ESI-MS *m/z*: 292 $(M + H - {}^tBu)^+$.

*tert-Butyl 3-(4-Methoxybenzyl)-6,6a-dihydro-3aH-pyrrolo[3,4-d]isoxazole-5(4H)-carboxylate (**13j**)*[76]. Pale-yellow oil, 64% yield. ^{1}H NMR (300 MHz, $CDCl_3$): δ 7.15 (d, J = 8.5 Hz, 2H), 6.88 (d, J = 8.5 Hz, 2H), 5.07 (ddd, J = 9.1, 5.8, 1.6 Hz, 1H), 3.80 (s, 3H), 3.85−3.75 (m, 2H), 3.60−3.40 (m, 4H), 3.30 (dd, J = 11.8, 8.5 Hz, 1H), 1.45 (s, 9H). ESI-MS *m/z*: 355 $(M + Na)^+$.

*tert-Butyl 3-(4-(tert-Butoxycarbonyl)phenyl)-6,6a-dihydro-3aH-pyrrolo[3,4-d]isoxazole-5(4H)-carboxylate (**13l**).* White solid, 69% yield; mp (EtOAc/hexane) 143−145 °C. ^{1}H NMR (300 MHz, $CDCl_3$): δ 8.02 (d, J = 8.2 Hz, 2H), 7.67 (d, J = 8.2 Hz, 2H), 5.34 (dd, J = 9.4, 5.6 Hz, 1H), 4.27−4.18 (m, 1 H), 4.00 (d, J = 12.9 Hz, 1H), 3.80−3.58 (m, 3H), 1.65 (s, 9H), 1.40 (s, 9H). ESI-MS *m/z*: 389 $(M + H)^+$.

General Procedure for the Synthesis of 5-Methyl-3-substituted-4,5,6,6a-tetrahydro-3a*H*-pyrrolo[3,4-*d*]isoxazoles (Compounds 8a−d, 8h−j, 8l). A solution of the proper *N*-Boc-protected derivative **13** (1.00 mmol) in 4 M HCl solution in dioxane (5.0 mL, 20.0 mmol) was stirred for 1 h and then concentrated in vacuo. The residue was treated with water (10 mL) and washed with CH_2Cl_2 twice. The aqueous phase was basified with $NaHCO_3$ and extracted with EtOAc (3 × 30 mL). The combined organic phases were washed with brine (10 mL), dried (Na_2SO_4), filtered, and concentrated in vacuo to afford the crude, unprotected derivative, which was used for the next step without further purification.

To a solution of the proper unprotected 4,5,6,6a-tetrahydro-3a*H*-pyrrolo[3,4-*d*]isoxazole (0.80 mmol) in acetone (8 mL), K_2CO_3 (442 mg, 3.20 mmol) and methyl iodide (49 μL, 0.80 mmol) were added. The resulting mixture was stirred at room temperature for 12 h, the solid was filtered off, and the solvent was evaporated. The residue was purified by silica gel chromatography (CH_2Cl_2/MeOH) to give the title compounds. Derivatives **8a−d** were recrystallized from the appropriate solvent. Compounds **8h** and **8i** were converted in the corresponding hydrochloride salts following the general procedure described for compounds **7a,b** and **7h−j**. Compound **8j** (53.0 mg, 0.21 mmol) was dissolved in EtOH (3 mL), and a solution of oxalic acid (30.0 mg, 0.24 mmol) in EtOH (1 mL) was added. The mixture was stirred at room temperature for 10 min, and the resulting solid was recrystallized from EtOH/Et_2O to yield title compounds as oxalate salt.

*5-Methyl-3-phenyl-4,5,6,6a-tetrahydro-3aH-pyrrolo[3,4-d]isoxazole (**8a**).* White solid, 48% yield; mp (EtOAc/hexane) 119−121 °C (decomp). ^{1}H NMR (300 MHz, $CDCl_3$): δ 7.68 (m, 2H), 7.40 (m, 3H), 5.22 (dd, J = 9.1, 4.5 Hz, 1H), 4.21−4.16 (m, J = 9.1, 7.4, 1.7 Hz, 1H), 3.26 (d, J = 11.0 Hz, 1H), 3.09 (d, J = 9.6 Hz, 1H), 2.51 (dd, J = 9.6, 7.4 Hz, 1H), 2.45 (dd, J = 11.0, 4.5 Hz, 1H), 2.33 (s, 3H). ESI-MS *m/z*: 203 $(M + H)^+$. Anal. ($C_{12}H_{14}N_2O$) C, H, N.

*5-Methyl-3-(4-nitrophenyl)-4,5,6,6a-tetrahydro-3aH-pyrrolo[3,4-d]isoxazole (**8b**).* White solid, 38% yield; mp (EtOAc/hexane) 161−162 °C. ^{1}H NMR (300 MHz, $CDCl_3$): δ 8.27 (d, J = 7.7 Hz, 2H), 7.85 (d, J = 7.7 Hz, 2H), 5.33 (dd, J = 4.3, 9.5, 1H), 4.23−4.17 (m, 1H), 3.33 (d, J = 11.2 Hz,

1H), 3.08 (d, J = 9.7, 1H), 2.66−2.43 (m, 2H), 2.37 (s, 3H). ESI-MS m/z: 248 $(M + H)^+$. Anal. ($C_{12}H_{13}N_3O_3$) C, H, N.

5-Methyl-3-(4-methoxyphenyl)-4,5,6,6a-tetrahydro-3aH-pyrrolo[3,4-d]isoxazole (***8c***). White solid, 33% yield; mp (EtOAc/hexane) 158−160 °C. ^{1}H NMR (300 MHz, $CDCl_3$): δ 7.61 (d, J = 8.8 Hz, 2H), 6.91 (d, J = 8.8 Hz, 2H), 5.19 (dd, J = 10.0, 4.6 Hz, 1H), 4.17−4.12 (m, 1H), 3.84 (s, 3H), 3.25 (d, J = 10.9 Hz, 1H), 3.07 (d, J = 9.0, 1H), 2.59−2.40 (m, 2H), 2.32 (s, 3H). ESI-MS m/z: 233 $(M + H)^+$. Anal. ($C_{13}H_{16}N_2O_2$) C, H, N.

5-Methyl-3-(4-(tosyloxy)phenyl)-4,5,6,6a-tetrahydro-3aH-pyrrolo-[3,4-d]isoxazole (***8d***). White solid, 32% yield; mp (EtOAc/hexane) 122−123 °C. ^{1}H NMR (300 MHz, $CDCl_3$): δ 7.70 (d, J = 8.5 Hz, 2H), 7.59 (d, J = 8.5 Hz, 2H), 7.32 (d, J = 8.5 Hz, 2H), 7.00 (d, J = 8.5 Hz, 2H), 5.22 (dd, J = 9.4, 4.1 Hz, 1H), 4.14−4.08 (m, 1H), 3.28 (d, J = 11.9 Hz, 1H), 3.07 (d, J = 9.4, 1H), 2.49−2.38 (m, 5H), 2.33 (s, 3H). ESI-MS m/z: 373 $(M + H)^+$. Anal. ($C_{19}H_{20}N_2O_4S$) C, H, N.

3-Benzyl-5-methyl-4,5,6,6a-tetrahydro-3aH-pyrrolo[3,4-d]isoxazole Hydrochloride (***8h***). White solid, 31% yield; mp (EtOH/Et_2O) 122−123 °C; free base. ^{1}H NMR (300 MHz, $CDCl_3$): δ 7.37−7.16 (m, 5H), 4.97 (dd, J = 4.6, 9.3 Hz, 1H), 3.89 (d, J = 15.1 Hz, 1H), 3.50 (d, J = 15.1 Hz, 1H), 3.55−3.42 (m, 1H), 3.20 (d, J = 10.9 Hz, 1H), 2.96 (d, J = 9.4 Hz, 1H), 2.31 (s, 3H), 2.26 (dd, J = 10.9, 4.6 Hz, 1H), 2.17 (dd, J = 9.4, 7.3 Hz, 1H). ESI-MS m/z: 217 $(M + H)^+$. Anal. ($C_{13}H_{16}N_2O\cdot HCl$) C, H, N.

5-Methyl-3-(4-nitrobenzyl)-4,5,6,6a-tetrahydro-3aH-pyrrolo[3,4-d] isoxazole Hydrochloride (***8i***). Pale-yellow solid, 40% yield; mp (EtOH/Et_2O) 239−240 °C (decomp); free base. ^{1}H NMR (300 MHz, $CDCl_3$): δ 8.20 (d, J = 8.5 Hz, 2H), 7.45 (d, J = 8.5 Hz, 2H), 5.03 (dd, J = 9.3, 4.6 Hz, 1H), 3.93 (d, J = 15.5 Hz, 1H), 3.64 (d, J = 15.5 Hz, 1H), 3.55−3.45 (m, 1H), 3.23 (d, J = 10.9 Hz, 1H), 2.94 (d, J = 9.7 Hz, 1H), 2.31 (s, 3H), 2.27 (dd, J = 10.9, 4.6 Hz, 1H), 2.20 (dd, J = 9.7, 7.2 Hz, 1H). ESI-MS m/z: 262 $(M + H)^+$. Anal. ($C_{13}H_{15}N_3O_3\cdot HCl$) C, H, N.

3-(4-Methoxybenzyl)-5-methyl-4,5,6,6a-tetrahydro-3aH-pyrrolo-[3,4-d]isoxazole Oxalate (***8j***). White solid, 34% yield; mp (Et_2O/EtOH) 138−140 °C; free base. ^{1}H NMR (300 MHz, $CDCl_3$): δ 7.14 (d, J = 8.4 Hz, 2H), 6.83 (d, J = 8.4 Hz, 2H), 4.94 (dd, J = 9.2, 4.6 Hz, 1H), 3.86−3.75 (m, 1H), 3.77 (s, 3H), 3.53−3.39 (m, 2H), 3.17 (d, J = 10.9 Hz, 1H), 2.93 (d, J = 9.4 Hz, 1H), 2.29 (s, 3H), 2.23 (dd, J = 10.9, 4.6 Hz, 1H), 2.14 (dd, J = 9.4, 7.4 Hz, 1H). ESI-MS m/z: 247 $(M + H)^+$. Anal. ($C_{14}H_{18}N_2O_2\cdot H_2CO_4$) C, H, N.

5-Methyl-3-(4-(tert-butoxycarbonyl)phenyl)-4,5,6,6a-tetrahydro-3aH-pyrrolo[3,4-d]isoxazole (***8l***). Colorless oil, 45% yield. ^{1}H NMR (300 MHz, $CDCl_3$): δ 8.00 (d, J = 8.8 Hz, 2H), 7.70 (d, J = 8.8 Hz, 2H), 5.25 (dd, J = 9.6, 4.4 Hz, 1H), 4.22−4.15 (m, 1H), 3.28 (d, J = 11.0 Hz, 1H), 3.06 (d, J = 9.3 Hz, 1H), 2.51 (dd, J = 9.3, 7.4 Hz, 1H), 2.45 (dd, J = 11.0, 4.4 Hz, 1H), 2.32 (s, 3 H), 1.58 (s, 9 H). ESI-MS m/z: 303 $(M + H)^+$.

3-(4-Hydroxyphenyl)-5-methyl-4,5,6,6a-tetrahydro-3a*H*-pyrrolo[3,4-*d*]isoxazole (8g). Deprotection of compound **8d** (70.0 mg, 0.19 mmol) according to the procedure used for **7g** yielded the title compound as a white solid (40.5 mg, 95%), which was recrystallized from EtOAc/hexane; mp 126−127 °C. ^{1}H NMR (300 MHz, DMSO-d_6): δ 9.87 (s, 1H), 7.46 (d, J = 8.5 Hz, 2H), 6.79 (d, J = 8.5 Hz, 2H), 5.05 (dd, J = 9.4, 4.3 Hz, 1H), 4.25−4.20 (m, 1H), 3.01 (d, J = 10.8 Hz, 1H), 2.85 (d, J = 9.5 Hz, 1H), 2.33 (dd, J = 9.5, 7.4 Hz, 1H), 2.25 (dd, J = 10.8, 4.3 Hz, 1H), 2.15 (s, 3H). ESI-MS m/z: 219 $(M + H)^+$. Anal. ($C_{12}H_{14}N_2O_2$) C, H, N.

3-(4-Aminophenyl)-5-methyl-4,5,6,6a-tetrahydro-3a*H*-pyrrolo[3,4-*d*]isoxazole Hydrochloride (8f). Reduction of compound **8b** (135 mg, 0.55 mmol) according to the procedure used for **7l** yielded the free amine (101 mg, 85%), which was converted to the hydrochloride salt following the general procedure described for compounds **7a**,**b**, and **7h**−**j**. White solid; mp (EtOH/Et_2O) 211−212 °C (decomp); free base. ^{1}H NMR (300 MHz, $CDCl_3$): δ 7.47 (d, J = 8.5 Hz, 2H), 6.67 (d, J = 8.5 Hz, 2H), 5.15 (dd, J = 9.3, 4.4 Hz, 1H), 4.15−4.08 (m, 1H), 3.87 (br s, 2H), 3.22 (d, J = 10.7 Hz, 1H), 3.06 (d, J = 9.6 Hz, 1H), 2.55−2.40 (m, 2H), 2.32 (s, 3H). ESI-MS m/z: 218 $(M + H)^+$. Anal. ($C_{12}H_{15}N_3O\cdot HCl$) C, H, N.

3-(4-Aminobenzyl)-5-methyl-4,5,6,6a-tetrahydro-3a*H*-pyrrolo[3,4-*d*]isoxazole oxalate (8k). Reduction of compound **8i** (140 mg, 0.54 mmol) according to the procedure used for **7f** yielded the free amine (103 mg, 83%), which was converted to the oxalate salt following the general procedure described for compound **8j**. White solid; mp (EtOH/Et_2O) 164−165 °C; free base. ^{1}H NMR (300 MHz, $CDCl_3$): δ 7.02 (d, J = 8.5 Hz, 2H), 6.64 (d, J = 8.5 Hz, 2H), 4.96 (dd, J = 9.3, 4.6 Hz, 1H), 3.77 (d, J = 15.1 Hz, 1H), 3.64 (br s, 2H), 3.49 (dd, 9.3, 7.5 Hz, 1H), 3.38 (d, J = 15.1 Hz, 1H), 3.19 (d, J = 10.9 Hz, 1H), 2.94 (d, J = 9.7 Hz, 1H), 2.31 (s, 3H), 2.31−2.25 (m, 1H), 2.18 (dd, J = 9.7, 7.5 Hz, 1H). ESI-MS m/z: 232 $(M + H)^+$. Anal. ($C_{13}H_{17}N_3O\cdot H_2CO_4$) C, H, N.

3-(4-Carboxyphenyl)-5-methyl-4,5,6,6a-tetrahydro-3a*H*-pyrrolo[3,4-*d*]isoxazole (8e). Deprotection of compound **8l** (200 mg, 0.66 mmol) according to the procedure used for **7e** yielded the title compounds (162 mg, 99%). White solid; mp (methanol/H_2O) 255−257 °C dec. ^{1}H NMR (300 MHz, DMSO-d_6): δ 10.20 (br s, 1H), 8.02 (d, J = 8.5 Hz, 2 H), 7.84 (d, J = 8.5 Hz, 2H), 5.50 (dd, J = 9.6, 4.4 Hz, 1H), 4.82−4.70 (m, 1H), 3.98−3.80 (m, 1H), 3.78−3.60 (m, 1H), 3.58−3.25 (m, 2H), 2.78 (s, 3H). ESI-MS m/z: 247 $(M + H)^+$. Anal. ($C_{13}H_{14}N_2O_3$) C, H, N.

DNMT1 Expression, Purification, and Assay. *Cloning and Purification of Recombinant DNMT1.* DNMT1 was produced and purified as described before.[55] Briefly, proteins were expressed in Sf9 insect cells (derived from *Spodoptera frugiperda*) and purified by affinity chromatography and gel filtration. The protein concentration of purified DNMT was determined by Bradford assay and verified by using Coomassie blue stained SDS/polyacrylamide gels and suitable molecular mass markers of known concentration. Protein identity was confirmed by immunoblotting using a DNMT1-specific antibody (Santa Cruz) according to the manufacturer's protocol.

Biochemical DNMT Activity Assay and Dose−Response Assays. DNA methylation assays were carried out in total reaction volume of 25 μL containing 0.4 μM hemimethylated or unmethylated oligonucleotide substrate purchased from MWG (upper strand: 5′-GATCGCXGATGCGXGAATXGCGATXGATGCGAT-3′, X = 5mC for hemimethylated or X = C for unmethylated substrate, and lower strand: 5′-ATCGCATCGATCGCGATTCGCGCATCGGCGATC-3′), purified DNMT (500 nM) in reaction buffer (100 mM KCl, 10 mM TrisCl pH 7.5, 1 mM EDTA), and BSA (1 mg/mL). All reactions were carried out at 37 °C in the presence of 0.7 μM [methyl-^{3}H] AdoMet (2.6 TBq/mmol, PerkinElmer). After 3 h, the reaction was stopped by adding 10 μL of 20% SDS and spotting of the whole volume onto DE81 cellulose paper. Filters were baked at 80 °C for 2 h and washed three times with cold 0.2 M NH_4HCO_3, three times with distilled water, and once with 100% ethanol. After drying, filters were transferred into Mini-Poly Q vial (PerkinElmer) and 5 mL of Ultima Gold LSC Cocktail was added per vial. Analysis was done in a scintillation counter, each measurement was repeated once.

Competition Assay. For the determination of the mode of action of **7b** in the catalytic domain of DNMT1, we used the model of Lai and Wu[78] as recommended by the NIH Chemical Genomics Center (http://www.ncgc.nih.gov/guidance) and adapted it to our biochemical DNMT activity assay. The conditions of the biochemical DNMT activity assay (see above) were slightly modified for the competition experiments: the inhibitor concentration was held constant at 150 μM, the reaction time at 37 °C was decreased to 1 h. The concentrations of either SAM substrate or oligo substrate were increased to test for competition with **7b**, which should result in a decreasing inhibition.

Cell Culture. HCT116 cells were obtained directly from the American Type Culture Collection (ATCC, www.atcc.org) and passaged in our

laboratory for fewer than 6 months after resuscitation. HCT116 were cultured in DMEM/Ham's F12 (BIOCHROM) supplemented with 10% FCS (Invitrogen). Cell proliferation and viability was assessed by counting trypan blue stained cells by TC10 automated cell counter (Bio-Rad).

Compounds. SAH, **2** and procaine were purchased by Sigma-Aldrich, and both were dissolved in water to 50 mM stocks and stored in aliquots at −80 °C.

Molecular Modeling. To conduct the docking studies, the protonated and neutral states of the *R* and *S* enantiomers of **7b** were prepared using Molecular Operating Environment (MOE), version 2008.10.[89] The crystal structure of human DNMT1 bound to SAH was retrieved from the Protein Data Bank (PDB entry 3PTA).[75] Docking was performed with the methyltransferase domain using the Glide (Grid-Based Ligand Docking with Energetics) program, version 5.7.[83,84] The Protein Preparation Wizard module of Maestro was used to prepare the protein[90] as we reported previously for other systems.[91] For docking, the scoring grids were centered on the crystal structure of SAH using the default bounding sizes, with an inner box of 10 Å on each side and an outer box of 25.4 Å on each side. Flexible docking with default parameters was used. Glide XP (Extra Precision) was employed for all docking calculations.[84] The best docked poses were selected as the ones with the lowest GlideScore; the more negative the Glide Score, the more favorable the binding.

■ ASSOCIATED CONTENT

Supporting Information. Elemental analysis for compounds **7a**−**k** and **8a**−**k**, characterization data of compounds **9a**−**d**, **9h**−**j**, **9l**, **12a**−**d**, **12h**−**j**, and **12l**. This material is available free of charge via the Internet at http://pubs.acs.org.

■ AUTHOR INFORMATION

Corresponding Author

*For D.K.: phone, +49-6221-42-3800; E-mail, d.kuck@dkfz.de. For J.L.M-F.: phone/fax, +1-772-345-4685; E-mail, jmedina@tpims.org. For G.S.: phone, +39-089-96-9770; fax, +39-089-96-9602; E-mail: gsbardella@unisa.it.

Author Contributions

⊥These two authors contributed equally to this work.

■ ACKNOWLEDGMENT

This work was supported by grants from Ministero dell'Università e della Ricerca Scientifica e Tecnologica—PRIN 2008 (S.C.), Università di Salerno (G.S.), COST Action TD09/05 Epigenetics (G.S.), Università degli Studi di Milano (P.C., A. P., L.T.), the State of Florida (J.L.M.-F.), and the Menopause & Women's Health Research Center (J.L.M.-F.). D.K. thanks Sara Myers for technical assistance with the DNMT1 activity assay. M. V. was supported by Università di Salerno with predoctoral fellowships.

■ ABBREVIATIONS USED

DMEM, Dulbecco's Modified Eagle's Medium; DNMT, DNA methyltransferase; FCS, fetal calf serum; HCT116, human colon carcinoma cell line; SAH, *S*-adenosyl-L-homocysteine; SAM, *S*-adenosyl methionine; Sf9, insect cell line derived from *Spodoptera frugiperda*; MOI, multiplicity of infection

■ REFERENCES

(1) Sharma, S.; Kelly, T. K.; Jones, P. A. Epigenetics in cancer. *Carcinogenesis* **2010**, *31*, 27–36.

(2) Jones, P. A.; Baylin, S. B. The Epigenomics of Cancer. *Cell* **2007**, *128*, 683–692.

(3) Esteller, M. Epigenetics in Cancer. *N. Engl. J. Med.* **2008**, *358*, 1148–1159.

(4) Portela, A.; Esteller, M. Epigenetic modifications and human disease. *Nature Biotechnol.* **2010**, *28*, 1057–1068.

(5) Bernstein, B. E.; Meissner, A.; Lander, E. S. The Mammalian Epigenome. *Cell* **2007**, *128*, 669–681.

(6) Kouzarides, T. Chromatin Modifications and Their Function. *Cell* **2007**, *128*, 693–705.

(7) Suzuki, M. M.; Bird, A. DNA methylation landscapes: provocative insights from epigenomics. *Nature Rev. Genet.* **2008**, *9*, 465–476.

(8) Feinberg, A. P.; Ohlsson, R.; Henikoff, S. The epigenetic progenitor origin of human cancer. *Nature Rev. Genet.* **2006**, *7*, 21–33.

(9) Jones, P. A.; Martienssen, R. A Blueprint for a Human Epigenome Project: The AACR Human Epigenome Workshop. *Cancer Res.* **2005**, *65*, 11241–11246.

(10) Bird, A. DNA methylation patterns and epigenetic memory. *Genes Dev.* **2002**, *16*, 6–21.

(11) Yoo, C. B.; Jones, P. A. Epigenetic therapy of cancer: past, present and future. *Nature Rev. Drug Discovery* **2006**, *5*, 37–50.

(12) In addition to 5-methylcytosines, 5-hydroxymethyl-2′-deoxycytidine has also been observed, although it seems not to be present in cancer cell lines. These new DNA modifications need to be further studied to determine their implications for normal and diseased epigenetic regulation. See: Kriaucionis, S.; Heintz, N. The Nuclear DNA Base 5-Hydroxymethylcytosine Is Present in Purkinje Neurons and the Brain. *Science* **2009**, *324*, 929–930.

(13) Non-CG methylation has recently been described in humans at CHG and CHH sites (where H is A, C or T). CHG and CHH methylation has been found in stem cells and the levels of non-CpG methylation decrease during differentiation and are restored in induced pluripotent stem cells, suggesting a key role in origin and maintenance of pluripotent state. Mechanisms of non-CpG methylation remain unclear. See: Lister, R.; Pelizzola, M.; Dowen, R. H.; Hawkins, R. D.; Hon, G.; Tonti-Filippini, J.; Nery, J. R.; Lee, L.; Ye, Z.; Ngo, Q. M.; Edsall, L.; Antosiewicz-Bourget, J.; Stewart, R.; Ruotti, V.; Millar, A. H.; Thomson, J. A.; Ren, B.; Ecker, J. R. Human DNA methylomes at base resolution show widespread epigenomic differences. *Nature* **2009**, *462*, 315–322. Laurent, L.; Wong, E.; Li, G.; Huynh, T.; Tsirigos, A.; Ong, C. T.; Low, H. M.; Kin Sung, K. W.; Rigoutsos, I.; Loring, J.; Wei, C.-L. Dynamic changes in the human methylome during differentiation. *Genome Res.* **2010**, *20*, 320–321.

(14) Esteller, M. Epigenetics in evolution and disease. *Lancet* **2008**, *372*, S90–S96.

(15) Doi, A.; Park, I.-H.; Wen, B.; Murakami, P.; Aryee, M. J.; Irizarry, R.; Herb, B.; Ladd-Acosta, C.; Rho, J.; Loewer, S.; Miller, J.; Schlaeger, T.; Daley, G. Q.; Feinberg, A. P. Differential methylation of tissue- and cancer-specific CpG island shores distinguishes human induced pluripotent stem cells, embryonic stem cells and fibroblasts. *Nature Genet.* **2009**, *41*, 1350–1353.

(16) Irizarry, R. A.; Ladd-Acosta, C.; Wen, B.; Wu, Z.; Montano, C.; Onyango, P.; Cui, H.; Gabo, K.; Rongione, M.; Webster, M.; Ji, H.; Potash, J. B.; Sabunciyan, S.; Feinberg, A. P. The human colon cancer methylome shows similar hypo- and hypermethylation at conserved tissue-specific CpG island shores. *Nature Genet.* **2009**, *41*, 178–186.

(17) Balch, C.; Nephew, K. P.; Huang, T. H. M.; Bapat, S. A. Epigenetic "bivalently marked" process of cancer stem cell-driven tumorigenesis. *Bioessays* **2007**, *29*, 842–845.

(18) Hewagama, A.; Richardson, B. The genetics and epigenetics of autoimmune diseases. *J. Autoimmun.* **2009**, *33*, 3–11.

(19) Liu, L.; van Groen, T.; Kadish, I.; Tollefsbol, T. O. DNA methylation impacts on learning and memory in aging. *Neurobiol. Aging* **2009**, *30*, 549–560.

(20) Ohm, J. E.; McGarvey, K. M.; Yu, X.; Cheng, L.; Schuebel, K. E.; Cope, L.; Mohammad, H. P.; Chen, W.; Daniel, V. C.; Yu, W.; Berman, D. M.; Jenuwein, T.; Pruitt, K.; Sharkis, S. J.; Watkins, D. N.; Herman, J. G.; Baylin, S. B. A stem cell-like chromatin pattern may predispose tumor suppressor genes to DNA hypermethylation and heritable silencing. *Nature Genet.* **2007**, *39*, 237–242.

(21) Richardson, B. Primer: epigenetics of autoimmunity. *Nature Clin. Pract. Rheum.* **2007**, *3*, 521–527.

(22) A fourth enzyme previously known as DNMT2 has strong sequence similarities with 5-methylcytosine methyltransferases but does not methylate DNA and was shown to methylate position 38 in aspartic acid transfer RNA. To better reflect its biological function, the name for this enzyme has been changed to tRNA aspartic acid methyltransferase 1 (TRDMT1). See: Goll, M. G.; Kirpekar, F.; Maggert, K. A.; Yoder, J. A.; Hsieh, C.-L.; Zhang, X.; Golic, K. G.; Jacobsen, S. E.; Bestor, T. H. Methylation of tRNAAsp by the DNA Methyltransferase Homolog Dnmt2. *Science* **2006**, *311*, 395–398.

(23) Goll, M. G.; Bestor, T. H. Eukaryotic cytosine methyltransferases. *Annu. Rev. Biochem.* **2005**, *74*, 481–514.

(24) Egger, G.; Liang, G.; Aparicio, A.; Jones, P. A. Epigenetics in human disease and prospects for epigenetic therapy. *Nature* **2004**, *429*, 457–463.

(25) Mai, A.; Altucci, L. Epi-drugs to fight cancer: from chemistry to cancer treatment, the road ahead. *Int. J. Biochem. Cell Biol.* **2009**, *41*, 199–213.

(26) Yoo, C. B.; Jeong, S.; Egger, G.; Liang, G.; Phiasivongsa, P.; Tang, C.; Redkar, S.; Jones, P. A. Delivery of 5-Aza-2′-Deoxycytidine to Cells Using Oligodeoxynucleotides. *Cancer Res.* **2007**, *67*, 6400–6408.

(27) Chuang, J. C.; Warner, S. L.; Vollmer, D.; Vankayalapati, H.; Redkar, S.; Bearss, D. J.; Qiu, X.; Yoo, C. B.; Jones, P. A. S110, a 5-Aza-2′-Deoxycytidine-Containing Dinucleotide, Is an Effective DNA Methylation Inhibitor In Vivo and Can Reduce Tumor Growth. *Mol. Cancer Ther.* **2010**, *9*, 1443–1450.

(28) Brueckner, B.; Lyko, F. DNA methyltransferase inhibitors: old and new drugs for an epigenetic cancer therapy. *Trends Pharmacol. Sci.* **2004**, *25*, 551–554.

(29) Brueckner, B.; Kuck, D.; Lyko, F. DNA Methyltransferase Inhibitors for Cancer Therapy. *Cancer J.* **2007**, *13*, 17–22.

(30) Lyko, F.; Brown, R. DNA Methyltransferase Inhibitors and the Development of Epigenetic Cancer Therapies. *J. Natl. Cancer Inst.* **2005**, *97*, 1498–1506.

(31) Stresemann, C.; Lyko, F. Modes of action of the DNA methyltransferase inhibitors azacytidine and decitabine. *Int. J. Cancer* **2008**, *123*, 8–13.

(32) Fang, M. Z.; Wang, Y.; Ai, N.; Hou, Z.; Sun, Y.; Lu, H.; Welsh, W.; Yang, C. S. Tea Polyphenol (−)-Epigallocatechin-3-Gallate Inhibits DNA Methyltransferase and Reactivates Methylation-Silenced Genes in Cancer Cell Lines. *Cancer Res.* **2003**, *63*, 7563–7570.

(33) Liu, Z.; Xie, Z.; Jones, W.; Pavlovicz, R. E.; Liu, S.; Yu, J.; Li, P.-k.; Lin, J.; Fuchs, J. R.; Marcucci, G.; Li, C.; Chan, K. K. Curcumin is a potent DNA hypomethylation agent. *Bioorg. Med. Chem. Lett.* **2009**, *19*, 706–709.

(34) Fini, L.; Selgrad, M.; Fogliano, V.; Graziani, G.; Romano, M.; Hotchkiss, E.; Daoud, Y. A.; De Vol, E. B.; Boland, C. R.; Ricciardiello, L. Annurca Apple Polyphenols Have Potent Demethylating Activity and Can Reactivate Silenced Tumor Suppressor Genes in Colorectal Cancer Cells. *J. Nutr.* **2007**, *137*, 2622–2628.

(35) Lee, W. J.; Zhu, B. T. Inhibition of DNA methylation by caffeic acid and chlorogenic acid, two common catechol-containing coffee polyphenols. *Carcinogenesis* **2006**, *27*, 269–277.

(36) Fang, M. Z.; Chen, D.; Sun, Y.; Jin, Z.; Christman, J. K.; Yang, C. S. Reversal of Hypermethylation and Reactivation of p16INK4a, RARβ, and MGMT Genes by Genistein and Other Isoflavones from Soy. *Clin. Cancer Res.* **2005**, *11*, 7033–7041.

(37) Pina, I. C.; Gautschi, J. T.; Wang, G.-Y.-S.; Sanders, M. L.; Schmitz, F. J.; France, D.; Cornell-Kennon, S.; Sambucetti, L. C.; Remiszewski, S. W.; Perez, L. B.; Bair, K. W.; Crews, P. Psammaplins from the Sponge *Pseudoceratina purpurea*: Inhibition of Both Histone Deacetylase and DNA Methyltransferase. *J. Org. Chem.* **2003**, *68*, 3866–3873.

(38) Brueckner, B.; Garcia Boy, R.; Siedlecki, P.; Musch, T.; Kliem, H. C.; Zielenkiewicz, P.; Suhai, S.; Wiessler, M.; Lyko, F. Epigenetic Reactivation of Tumor Suppressor Genes by a Novel Small-Molecule Inhibitor of Human DNA Methyltransferases. *Cancer Res.* **2005**, *65*, 6305–6311.

(39) Siedlecki, P.; Garcia Boy, R.; Musch, T.; Brueckner, B.; Suhai, S.; Lyko, F.; Zielenkiewicz, P. Discovery of Two Novel, Small-Molecule Inhibitors of DNA Methylation. *J. Med. Chem.* **2006**, *49*, 678–683.

(40) Suzuki, T.; Tanaka, R.; Hamada, S.; Nakagawa, H.; Miyata, N. Design, synthesis, inhibitory activity, and binding mode study of novel DNA methyltransferase 1 inhibitors. *Bioorg. Med. Chem. Lett.* **2010**, *20*, 1124–1127.

(41) Kuck, D.; Caulfield, T.; Lyko, F.; Medina-Franco, J. L. Nanaomycin A Selectively Inhibits DNMT3B and Reactivates Silenced Tumor Suppressor Genes in Human Cancer Cells. *Mol. Cancer Ther.* **2010**, *9*, 3015–3023.

(42) Lin, R.-K.; Hsu, C.-H.; Wang, Y.-C. Mithramycin A inhibits DNA methyltransferase and metastasis potential of lung cancer cells. *Anti-Cancer Drugs* **2007**, *18*, 1157–1164.

(43) Isakovic, L.; Saavedra, O. M.; Llewellyn, D. B.; Claridge, S.; Zhan, L.; Bernstein, N.; Vaisburg, A.; Elowe, N.; Petschner, A. J.; Rahil, J.; Beaulieu, N.; Gauthier, F.; MacLeod, A. R.; Delorme, D.; Besterman, J. M.; Wahhab, A. Constrained L-)-*S*-adenosyl-L-homocysteine (SAH) analogues as DNA methyltransferase inhibitors. *Bioorg. Med. Chem. Lett.* **2009**, *19*, 2742–2746.

(44) Saavedra, O. M.; Isakovic, L.; Llewellyn, D. B.; Zhan, L.; Bernstein, N.; Claridge, S.; Raeppel, F.; Vaisburg, A.; Elowe, N.; Petschner, A. J.; Rahil, J.; Beaulieu, N.; MacLeod, A. R.; Delorme, D.; Besterman, J. M.; Wahhab, A. SAR around L)-*S*-adenosyl-L-homocysteine, an inhibitor of human DNA methyltransferase (DNMT) enzymes. *Bioorg. Med. Chem. Lett.* **2009**, *19*, 2747–2751.

(45) Lin, Y.-S.; Shaw, A.; Wang, S.-G.; Hsu, C.-C.; Teng, I.-W.; Tseng, M.-J.; Huang, T.; Chen, C.-S.; Leu, Y.-W.; Hsiao, S.-H. Identification of novel DNA methylation inhibitors via a two-component reporter gene system. *J. Biomed. Sci.* **2011**, *18*, 3.

(46) Datta, J.; Ghoshal, K.; Denny, W. A.; Gamage, S. A.; Brooke, D. G.; Phiasivongsa, P.; Redkar, S.; Jacob, S. T. A New Class of Quinoline-Based DNA Hypomethylating Agents Reactivates Tumor Suppressor Genes by Blocking DNA Methyltransferase 1 Activity and Inducing Its Degradation. *Cancer Res.* **2009**, *69*, 4277–4285.

(47) Cornacchia, E.; Golbus, J.; Maybaum, J.; Strahler, J.; Hanash, S.; Richardson, B. Hydralazine and procainamide inhibit T cell DNA methylation and induce autoreactivity. *J. Immunol.* **1988**, *140*, 2197–2200.

(48) Singh, N.; Dueñas-González, A.; Lyko, F.; Medina-Franco, J. L. Molecular Modeling and Molecular Dynamics Studies of Hydralazine with Human DNA Methyltransferase 1. *ChemMedChem* **2009**, *4*, 792–799.

(49) Lin, X.; Asgari, K.; Putzi, M. J.; Gage, W. R.; Yu, X.; Cornblatt, B. S.; Kumar, A.; Piantadosi, S.; DeWeese, T. L.; De Marzo, A. M.; Nelson, W. G. Reversal of GSTP1 CpG Island Hypermethylation and Reactivation of π-Class Glutathione *S*-Transferase (GSTP1) Expression in Human Prostate Cancer Cells by Treatment with Procainamide. *Cancer Res.* **2001**, *61*, 8611–8616.

(50) Scheinbart, L. S.; Johnson, M. A.; Gross, L. A.; Edelstein, S. R.; Richardson, B. C. Procainamide inhibits DNA methyltransferase in a human T cell line. *J. Rheumatol.* **1991**, *18*, 530–534.

(51) Villar-Garea, A.; Fraga, M. F.; Espada, J.; Esteller, M. Procaine Is a DNA-Demethylating Agent with Growth-Inhibitory Effects in Human Cancer Cells. *Cancer Res.* **2003**, *63*, 4984–4989.

(52) Lee, B. H.; Yegnasubramanian, S.; Lin, X.; Nelson, W. G. Procainamide Is a Specific Inhibitor of DNA Methyltransferase 1. *J. Biol. Chem.* **2005**, *280*, 40749–40756.

(53) Kuck, D.; Singh, N.; Lyko, F.; Medina-Franco, J. L. Novel and selective DNA methyltransferase inhibitors: docking-based virtual screening and experimental evaluation. *Bioorg. Med. Chem.* **2010**, *18*, 822–829.

(54) Medina-Franco, J.; López-Vallejo, F.; Kuck, D.; Lyko, F. Natural products as DNA methyltransferase inhibitors: a computer-aided discovery approach. *Mol. Diversity* **2011**, *15*, 293–304.

(55) Castellano, S.; Kuck, D.; Sala, M.; Novellino, E.; Lyko, F.; Sbardella, G. Constrained analogues of procaine as novel small molecule inhibitors of DNA methyltransferase-1. *J. Med. Chem.* **2008**, *51*, 2321–2325.

(56) Massa, S.; Mai, A.; Sbardella, G.; Esposito, M.; Ragno, R.; Loidl, P.; Brosch, G. 3-(4-Aroyl-1*H*-pyrrol-2-yl)-*N*-hydroxy-2-propenamides, a New Class of Synthetic Histone Deacetylase Inhibitors. *J. Med. Chem.* **2001**, *44*, 2069–2072.

(57) Milite, C.; Castellano, S.; Benedetti, R.; Tosco, A.; Ciliberti, C.; Vicidomini, C.; Boully, L.; Franci, G.; Altucci, L.; Mai, A.; Sbardella, G. Modulation of the activity of histone acetyltransferases by long chain alkylidenemalonates (LoCAMs). *Bioorg. Med. Chem.* **2011**, *19*, 3690–3701.

(58) Piaz, F.; Vassallo, A.; Rubio, O.; Castellano, S.; Sbardella, G.; De Tommasi, N. Chemical biology of histone acetyltransferase natural compounds modulators. *Mol. Diversity* **2011**, *15*, 401–416.

(59) Dal Piaz, F.; Tosco, A.; Eletto, D.; Piccinelli, A. L.; Moltedo, O.; Franceschelli, S.; Sbardella, G.; Remondelli, P.; Rastrelli, L.; Vesci, L.; Pisano, C.; De Tommasi, N. The Identification of a Novel Natural Activator of p300 Histone Acetyltranferase Provides New Insights into the Modulation Mechanism of this Enzyme. *ChemBioChem* **2010**, *11*, 818–827.

(60) Castellano, S.; Milite, C.; Ragno, R.; Simeoni, S.; Mai, A.; Limongelli, V.; Novellino, E.; Bauer, I.; Brosch, G.; Spannhoff, A.; Cheng, D.; Bedford, M. T.; Sbardella, G. Design, Synthesis and Biological Evaluation of Carboxy Analogues of Arginine Methyltransferase Inhibitor 1 (AMI-1). *ChemMedChem* **2010**, *5*, 398–414.

(61) Sbardella, G.; Castellano, S.; Vicidomini, C.; Rotili, D.; Nebbioso, A.; Miceli, M.; Altucci, L.; Mai, A. Identification of long chain alkylidenemalonates as novel small molecule modulators of histone acetyltransferases. *Bioorg. Med. Chem. Lett.* **2008**, *18*, 2788–2792.

(62) Mai, A.; Rotili, D.; Tarantino, D.; Nebbioso, A.; Castellano, S.; Sbardella, G.; Tini, M.; Altucci, L. Identification of 4-hydroxyquinolines inhibitors of p300/CBP histone acetyltransferases. *Bioorg. Med. Chem. Lett.* **2009**, *19*, 1132–1135.

(63) Spannhoff, A.; Kim, Y. K.; Raynal, N. J. M.; Gharibyan, V.; Su, M.-B.; Zhou, Y.-Y.; Li, J.; Castellano, S.; Sbardella, G.; Issa, J.-P. J.; Bedford, M. T. Histone deacetylase inhibitor activity in royal jelly might facilitate caste switching in bees. *EMBO Rep.* **2011**, *12*, 238–243.

(64) Colussi, C.; Rosati, J.; Straino, S.; Spallotta, F.; Berni, R.; Stilli, D.; Rossi, S.; Musso, E.; Macchi, E.; Mai, A.; Sbardella, G.; Castellano, S.; Chimenti, C.; Frustaci, A.; Nebbioso, A.; Altucci, L.; Capogrossi, M. C.; Gaetano, C. *N*ε-Lysine acetylation determines dissociation from GAP junctions and lateralization of connexin 43 in normal and dystrophic heart. *Proc. Natl. Acad. Sci. U.S.A.* **2011**, *108*, 2795–2800.

(65) Mai, A.; Cheng, D.; Bedford, M. T.; Valente, S.; Nebbioso, A.; Perrone, A.; Brosch, G.; Sbardella, G.; De Bellis, F.; Miceli, M.; Altucci, L. Epigenetic Multiple Ligands: Mixed Histone/Protein Methyltransferase, Acetyltransferase, and Class III Deacetylase (Sirtuin) Inhibitors. *J. Med. Chem.* **2008**, *51*, 2279–2290.

(66) Mai, A.; Valente, S.; Cheng, D.; Perrone, A.; Ragno, R.; Simeoni, S.; Sbardella, G.; Brosch, G.; Nebbioso, A.; Conte, M.; Altucci, L.; Bedford, M. T. Synthesis and Biological Validation of Novel Synthetic Histone/Protein Methyltransferase Inhibitors. *ChemMedChem* **2007**, *2*, 987–991.

(67) Ragno, R.; Simeoni, S.; Castellano, S.; Vicidomini, C.; Mai, A.; Caroli, A.; Tramontano, A.; Bonaccini, C.; Trojer, P.; Bauer, I.; Brosch, G.; Sbardella, G. Small Molecule Inhibitors of Histone Arginine Methyltransferases: Homology Modeling, Molecular Docking, Binding Mode Analysis, and Biological Evaluations. *J. Med. Chem.* **2007**, *50*, 1241–1253.

(68) Mai, A.; Rotili, D.; Tarantino, D.; Ornaghi, P.; Tosi, F.; Vicidomini, C.; Sbardella, G.; Nebbioso, A.; Miceli, M.; Altucci, L.; Filetici, P. Small-Molecule Inhibitors of Histone Acetyltransferase Activity: Identification and Biological Properties. *J. Med. Chem.* **2006**, *49*, 6897–6907.

(69) Sbardella, G.; Bartolini, S.; Castellano, S.; Artico, M.; Paesano, N.; Rotili, D.; Spadafora, C.; Mai, A. 6-Alkylthio-4-[1-(2,6-difluorophenyl)alkyl]-1*H*-[1,3,5]triazin-2-ones (ADATs): Novel Regulators of Cell Differentiation and Proliferation. *ChemMedChem* **2006**, *1*, 1073–1080.

(70) Bartolini, S.; Mai, A.; Artico, M.; Paesano, N.; Rotili, D.; Spadafora, C.; Sbardella, G. 6-[1-(2,6-Difluorophenyl)ethyl]pyrimidinones Antagonize Cell Proliferation and Induce Cell Differentiation by Inhibiting (a Nontelomeric) Endogenous Reverse Transcriptase. *J. Med. Chem.* **2005**, *48*, 6776–6778.

(71) Ornaghi, P.; Rotili, D.; Sbardella, G.; Mai, A.; Filetici, P. A novel Gcn5p inhibitor represses cell growth, gene transcription and histone acetylation in budding yeast. *Biochem. Pharmacol.* **2005**, *70*, 911–917.

(72) Mai, A.; Massa, S.; Ragno, R.; Esposito, M.; Sbardella, G.; Nocca, G.; Scatena, R.; Jesacher, F.; Loidl, P.; Brosch, G. Binding Mode Analysis of 3-(4-Benzoyl-1-methyl-1*H*-2-pyrrolyl)-*N*-hydroxy-2-propenamide: A New Synthetic Histone Deacetylase Inhibitor Inducing Histone Hyperacetylation, Growth Inhibition, and Terminal Cell Differentiation. *J. Med. Chem.* **2002**, *45*, 1778–1784.

(73) Lu, Q.; Wu, A.; Richardson, B. C. Demethylation of the same promoter sequence increases CD70 expression in lupus T cells and T cells treated with lupus-inducing drugs. *J. Immunol.* **2005**, *174*, 6212–6219.

(74) Segura-Pacheco, B.; Trejo-Becerril, C.; Perez-Cardenas, E.; Taja-Chayeb, L.; Mariscal, I.; Chavez, A.; Acuña, C.; Salazar, A. M.; Lizano, M.; Dueñas-Gonzalez, A. Reactivation of tumor suppressor genes by the cardiovascular drugs hydralazine and procainamide and their potential use in cancer therapy. *Clin. Cancer Res.* **2003**, *9*, 1596–1603.

(75) Song, J.; Rechkoblit, O.; Bestor, T. H.; Patel, D. J. Structure of DNMT1−DNA Complex Reveals a Role for Autoinhibition in Maintenance DNA Methylation. *Science* **2011**, *331*, 1036–1040.

(76) Castellano, S.; Tamborini, L.; Viviano, M.; Pinto, A.; Sbardella, G.; Conti, P. Synthesis of 3-Aryl/benzyl-4,5,6,6a-tetrahydro-3a*H*-pyrrolo[3,4-*d*]isoxazole Derivatives: A Comparison between Conventional, Microwave-Assisted and Flow-Based Methodologies. *J. Org. Chem.* **2010**, *75*, 7439–7442.

(77) Recently, a fluorescence-based assay using a short DNA duplex immobilized on 96-well plates was employed to screen flavones and flavanones for the inhibition of murine catalytic Dnmt3a/3L.Ceccaldi, A.; Rajavelu, A.; Champion, C.; Rampon, C.; Jurkowska, R.; Jankevicius, G.; Sénamaud-Beaufort, C.; Ponger, L.; Gagey, N.; Dali Ali, H.; Tost, J.; Vriz, S.; Ros, S.; Dauzonne, D.; Jeltsch, A.; Guianvarc'h, D.; Arimondo, P. B. C5-DNA Methyltransferase Inhibitors: From Screening to Effects on Zebrafish Embryo Development. *ChemBioChem* **2011**, *12*, 1337–1345.

(78) Lai, C.-J.; Wu, J. C. A Simple Kinetic Method for Rapid Mechanistic Analysis of Reversible Enzyme Inhibitors. *Assay Drug Dev. Technol.* **2003**, *1*, 527–535.

(79) Yoo, J.; Medina-Franco, J. Homology modeling, docking and structure-based pharmacophore of inhibitors of DNA methyltransferase. *J. Comput.-Aided Mol. Des.* **2011**, *25*, 555–567.

(80) Medina-Franco, J. L.; Caulfield, T. Advances in the computational development of DNA methyltransferase inhibitors. *Drug Discovery Today* **2011**, *16*, 418–425.

(81) Yoo, J.; Medina-Franco, J. Trimethylaurintricarboxylic acid inhibits human DNA methyltransferase 1: insights from enzymatic and molecular modeling studies. *J. Mol. Model.* **2011**, DOI: 10.1007/s00894-011-1191-4. Published Online: July 29, 2011.

(82) Siedlecki, P.; Boy, R. G.; Comagic, S.; Schirrmacher, R.; Wiessler, M.; Zielenkiewicz, P.; Suhai, S.; Lyko, F. Establishment and functional validation of a structural homology model for human DNA methyltransferase 1. *Biochem. Biophys. Res. Commun.* **2003**, *306*, 558–563.

(83) *Glide*, version 5.7; Schrödinger, LLC: New York, NY, 2011.

(84) Friesner, R. A.; Murphy, R. B.; Repasky, M. P.; Frye, L. L.; Greenwood, J. R.; Halgren, T. A.; Sanschagrin, P. C.; Mainz, D. T. Extra Precision Glide: Docking and Scoring Incorporating a Model of Hydrophobic Enclosure for Protein−Ligand Complexes. *J. Med. Chem.* **2006**, *49*, 6177–6196.

(85) Jeltsch, A. Beyond Watson and Crick: DNA Methylation and Molecular Enzymology of DNA Methyltransferases. *ChemBioChem* **2002**, *3*, 274–293.

(86) Klimasauskas, S.; Kumar, S.; Roberts, R. J.; Cheng, X. Hhal methyltransferase flips its target base out of the DNA helix. *Cell* **1994**, *76*, 357–369.

(87) Rhee, I.; Bachman, K. E.; Park, B. H.; Jair, K.-W.; Yen, R.-W. C.; Schuebel, K. E.; Cui, H.; Feinberg, A. P.; Lengauer, C.; Kinzler, K. W.; Baylin, S. B.; Vogelstein, B. DNMT1 and DNMT3b cooperate to silence genes in human cancer cells. *Nature* **2002**, *416*, 552–556.

(88) Chen, T.; Hevi, S.; Gay, F.; Tsujimoto, N.; He, T.; Zhang, B.; Ueda, Y.; Li, E. Complete inactivation of DNMT1 leads to mitotic catastrophe in human cancer cells. *Nature Genet.* **2007**, *39*, 391–396.

(89) *Molecular Operating Environment (MOE)*, version 2008.10; Chemical Computing Group Inc.: Montreal, Quebec, Canada, 2008.

(90) *Schrödinger Suite 2011 Protein Preparation Wizard*, Epik version 2.2, Impact version 5.7, Prime version 3.0; Schrödinger, LLC: New York, NY, 2011.

(91) Hernández-Campos, A.; Velázquez-Martínez, I.; Castillo, R.; López-Vallejo, F.; Jia, P.; Yu, Y.; Giulianotti, M. A.; Medina-Franco, J. L. Docking of Protein Kinase B Inhibitors: Implications in the Structure-Based Optimization of a Novel Scaffold. *Chem. Biol. Drug Des.* **2010**, *76*, 269–276.